

# FLOW AND ELASTIC NETWORKS ON THE $N$ -TORUS: GEOMETRY, ANALYSIS, AND COMPUTATION\*

SABER JAFARPOUR<sup>†</sup>, ELIZABETH Y. HUANG<sup>†</sup>, KEVIN D. SMITH<sup>†</sup>, AND  
FRANCESCO BULLO<sup>†</sup>.

**Abstract.** Networks with phase-valued nodal variables are central in modeling several important societal and physical systems, including power grids, biological systems, and coupled oscillator networks. One of the distinctive features of phase-valued networks is the existence of multiple operating conditions corresponding to critical points of an energy function or feasible flows of a balance equation. For networks with phase-valued states, it is not yet fully understood how many operating conditions exist, how to characterize them, and how to compute them efficiently. A deeper understanding of feasible operating conditions, including their dependence upon network structures, may lead to more reliable and efficient network systems.

This paper introduces flow and elastic network problems on the  $n$ -torus and provides a rigorous and comprehensive framework for their study. Based on a monotonicity assumption, this framework localizes the solutions, bounds their number, and leads to an algorithm to compute them. Our analysis is based on a novel *winding partition* of the  $n$ -torus into winding cells, induced by *Kirchhoff's angle law* for undirected graphs. The winding partition has several useful properties, including that each winding cell contains at most one solution. The proposed algorithm is based on a novel contraction mapping and is guaranteed to compute all solutions. Finally, we apply our results to numerically study the active power flow equations in several test cases and estimate power transmission capacity and congestion of a power network.

**Key words.** Network systems, graph theory,  $n$ -torus, cycle structure of a graph

**AMS subject classifications.** 37C25, 93C10, 37C75, 37C65, 37N35

## 1. Introduction.

**Problem description and motivation.** Complex networks are ubiquitous in the natural and engineered world, arising in such disparate fields as biology, sociology, and infrastructure systems. In many networks of interest, the relevant quantities are represented as nodal and edge variables, and governing equations regulate their relationships and evolution. Nodal variables are typically real-valued and represent physical quantities, such as mass and density, or abstract quantities, such as information and opinions. Examples of engineered networks with real-valued nodal variables include water supply networks, gas distribution networks, and direct current (DC) power grids. However, in some important applications, nodal variables are more accurately modeled as phases, i.e., points on the circle  $\mathbb{T}^1$ . In these systems, the network state belongs to the  $n$ -torus  $\mathbb{T}^n$ , instead of the Euclidean space  $\mathbb{R}^n$ ; we refer to such systems as *networks on the  $n$ -torus*. Alternating-current (AC) power grids are well-known examples of networks on the  $n$ -torus, whereby power suppliers and consumers are the nodes and transmission lines are the edges. The operating condition of an AC power grid is described by the voltage angle at each node (nodal variables) and the power flow along each transmission line (edge variables). Other examples of networks on the  $n$ -torus arise in the study of synchronization of coupled oscillators and collective motion of multi-agent systems.

\*This work was supported in part by the Solar Energy Technologies Office of the U.S. Department of Energy under Contract No. DE-EE0000-1583 and by the Defense Threat Reduction Agency under Contract No. HDTRA1-19-1-0017. Figures 2–9 and 12 are licensed under Creative Commons Attribution-ShareAlike 4.0 International License (CC BY-SA 4.0) and are reproduced from [7].

<sup>†</sup>Center for Control, Dynamical Systems, and Computation and Department of Mechanical Engineering, University of California, Santa Barbara ([saber](mailto:saber), [eyhuang](mailto:eyhuang), [kevinsmith](mailto:kevinsmith), [bullo@ucsb.edu](mailto:bullo@ucsb.edu)).

In networks on the  $n$ -torus, solutions of the governing equations may be fixed-points of an algebraic equation, equilibrium points of a dynamical system, or critical points of an optimization problem. One of the distinctive behaviors of the network governing equations is the coexistence of multiple solutions. This behavior is observed in the existence of multiple stable operating conditions in AC power grids [9], diverse frequency-synchronized states in coupled oscillators [40], and rich spatial patterns of motion in engineered and biological networks [35]. Formally, determining the solutions to governing equations is often equivalent to computing zeros of continuous maps from  $\mathbb{T}^n$  to  $\mathbb{R}^n$ . And, indeed, the Poincaré–Hopf Theorem [48] forbids the uniqueness of such zeros. In all applications of networks on the  $n$ -torus, a comprehensive understanding of the multiplicity of solutions is critical for monitoring, predicting, and controlling the network system.

For systems with real-valued nodal variables, it is well-known that solutions to the network governing equations are related to structural properties of the network, and algebraic graph theory provides powerful tools for analyzing this relationship. However, for networks on the  $n$ -torus, the geometry of the ambient space complicates the connection between the structure of the network and its behavior. Despite numerous efforts in various scientific disciplines, many fundamental questions are not yet well understood: How many solutions exist? How can they be localized and computed? What is the role of the network structure? In this paper, we address these problems by developing a novel algebraic graph theory on the  $n$ -torus.

**Flow and elastic networks on the  $n$ -torus.** We introduce two classes of networks on the  $n$ -torus, namely *flow networks* and *elastic networks*, motivated by important example systems. We start with some notation. A network is described by a weighted undirected graph  $G$  with node set  $\{1, \dots, n\}$ , edge set  $\mathcal{E}$  of cardinality  $m$ , and edge weights  $a_{ij} \in \mathbb{R}_{>0}$ , for  $(i, j) \in \mathcal{E}$ . Given an arbitrary orientation and ordering of the edges, let  $B \in \mathbb{R}^{n \times m}$  denote the incidence matrix of  $G$ . We let  $\mathbb{T}^1$  denote the unit circle and  $\mathbb{T}^n$  denote the  $n$ -torus. Given angles  $\alpha, \beta \in \mathbb{T}^1$ , the geodesic distance between  $\alpha$  and  $\beta$ , denoted by  $|\alpha - \beta|$ , is the length of the shortest arc in  $\mathbb{T}^1$  connecting  $\alpha$  to  $\beta$ . If we identify  $\mathbb{T}^1 \simeq [-\pi, \pi)$ , the counterclockwise difference  $d_{cc}(\alpha, \beta)$  is defined by  $d_{cc}(\alpha, \beta) = \text{mod}((\beta - \alpha), 2\pi) - \pi$ . By abuse of notation, we write  $\alpha - \beta$  to refer to  $d_{cc}(\alpha, \beta)$ .  $\mathbf{1}_n$  and  $\mathbf{0}_n$  are the all-one and all-zero column vectors of length  $n$ , respectively, and  $\mathbf{1}_n^\perp$  is the subspace of  $\mathbb{R}^n$  consisting of vectors perpendicular to  $\mathbf{1}_n$ .

A flow network is characterized by a commodity being exchanged between adjacent nodes. The direction and magnitude of this flow is a function of the phase difference between adjacent nodes. Moreover, flows satisfy a balance equation asserting that, at each node, the total outflow (resp. inflow) must equal the supply (resp. demand) of commodity. The solutions of a flow network problem reveal the directions and magnitudes of commodity flows within the network, given the external supply and demand at each node.

**PROBLEM 1** (Flow networks on the  $n$ -torus). *A flow network on the  $n$ -torus is a pair  $(G, \{h_e\}_{e \in \mathcal{E}})$ , where  $G$  is a weighted undirected graph with  $n$  nodes and, for every  $e \in \mathcal{E}$ ,  $h_e : \mathbb{R} \rightarrow \mathbb{R}$  is a continuously differentiable  $2\pi$ -periodic odd function, called the flow function on edge  $e$ .*

*Consider a flow network on the  $n$ -torus  $(G, \{h_e\}_{e \in \mathcal{E}})$ , a balanced supply/demand vector  $p_{sd} \in \mathbf{1}_n^\perp$ , and an angle  $\gamma \in [0, \pi)$ . Then the flow network problem on the  $n$ -torus for  $(G, \{h_e\}_{e \in \mathcal{E}}, p_{sd}, \gamma)$  is to compute pairs of flows and phase angles  $(f, \theta) \in \mathbb{R}^m \times \mathbb{T}^n$*

such that

$$\begin{aligned}
 (1.1a) \quad & Bf = p_{\text{sd}}, \\
 (1.1b) \quad & f_e = a_{ij} h_e(\theta_i - \theta_j), \quad \text{for } e = (i, j) \in \mathcal{E} \\
 (1.1c) \quad & |\theta_i - \theta_j| \leq \gamma, \quad \text{for } (i, j) \in \mathcal{E}.
 \end{aligned}$$

These notions are illustrated in Figure 1 and interpreted as follows. Equation (1.1a) is the *flow balance equation* for a commodity flowing on a network, similar to a Kirchhoff's current conservation law, and is illustrated in Figure 1a. Equation (1.1b) is the *flow equation* and codifies how the flow along an edge is a function of the counter-clockwise difference between the angular variables at the two nodes; such a function is illustrated in Figure 1b. The oddness of the flow functions encodes the physical property that, on every edge, the flow equations are independent of the flow direction. Finally, the inequality (1.1c) is the *angle constraint*, often relevant in applications.

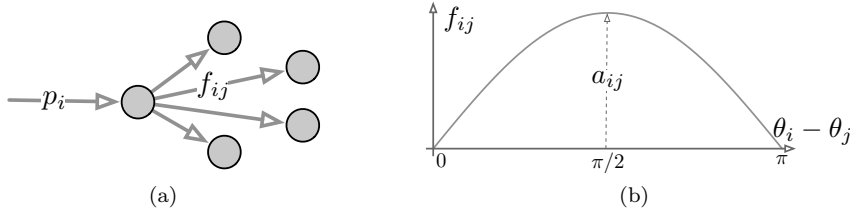


Fig. 1: Interpretation of the flow network problem (1.1) for the networks where the flow function has a sine form. Figure 1a illustrates that the flow satisfies a conservation law at each node:  $p_i = \sum_{j=1}^n f_{ij}$ . Figure 1b shows the proportional relationship between the flow transferred along each edge and the sine of its angle difference.

Flow networks on the  $n$ -torus arises in chemical oscillations [56, 33], where the commodity is mass. They also arise in models of AC power networks [4], droop-controlled inverters in microgrids [65], and networks of pacemaker cells in the heart [47], where the commodity is electricity. Models of brain networks [71], deep brain stimulation [67], and social influence systems [60] can also take the form of a flow network on the  $n$ -torus, with commodities like information and opinions.

An elastic networks is characterized by an interaction energy between adjacent nodes. The energy of an edge is a function of the phase difference between the adjacent nodes and these interaction energies give rise to forces on nodes. When an elastic network is in steady-state, the forces arising from these potential energies must cancel out with external forces, resulting in a force balance equation. The solutions of an elastic network reveal the possible steady-state energies and forces along edges, given external forces at each node.

**PROBLEM 2** (Elastic networks on the  $n$ -torus). *An elastic network on the  $n$ -torus is a pair  $(G, \{H_e\}_{e \in \mathcal{E}})$ , where  $G$  is a weighted undirected graph with  $n$  nodes and, for every edge  $e \in \mathcal{E}$ ,  $H_e : \mathbb{R} \rightarrow \mathbb{R}$  is a twice-differentiable  $2\pi$ -periodic even function called the elastic energy function of edge  $e$ . The elastic energy of the elastic network is*

$$(1.2) \quad \mathcal{H}(\theta) = \sum_{e=(i,j) \in \mathcal{E}} a_{ij} H_e(\theta_i - \theta_j).$$

*Consider an elastic network  $(G, \{H_e\}_{e \in \mathcal{E}})$ , a balanced torque vector  $\tau \in \mathbb{1}_n^\perp$ , and an angle  $\gamma \in [0, \pi)$ . Then the elastic network problem on the  $n$ -torus for  $(G, \{H_e\}_{e \in \mathcal{E}}, \tau, \gamma)$*

is to compute the phase angles  $\theta \in \mathbb{T}^n$  such that

$$(1.3a) \quad \tau = \nabla_{\theta} \mathcal{H}(\theta),$$

$$(1.3b) \quad |\theta_i - \theta_j| \leq \gamma, \quad \text{for } (i, j) \in \mathcal{E}.$$

These notions are illustrated in Figure (2) and interpreted as follows. For every edge  $e$ , the elastic energy function  $H_e$  codifies how the elastic energy in the edge  $e$  is a function of the counterclockwise difference between the angular variables at its end points. Equation (1.3a) is the *torque balance equation* for torques applied to a node in the network and is similar to conservation of momentum. Finally, the inequality (1.3b) is the *angle constraint*, often relevant in applications.

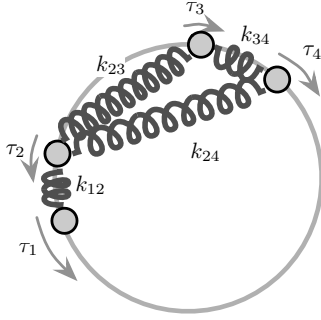


Fig. 2: Interpretation of the elastic network problem (1.3) as a spring network on a ring. Each particle on the ring is subject to an external torque, a damping torque, and is interconnected by ideal elastic springs to other particles.

Elastic networks on the  $n$ -torus are present in many engineering systems, including vehicle coordination [59, 63], nullforming in wireless networks [32], and nanoelectromechanical oscillator networks [41]. They arise in physics in the context of solid-state circuits [50], spin glass models [11], and Josephson junctions in quantum mechanics [73]. They can also model collective behavior in biological networks [72].

Elastic networks can also arise from certain network optimization problems on the  $n$ -torus, in which a cost function  $\mathcal{H} : \mathbb{T}^n \rightarrow \mathbb{R}$  can be decomposed into the sum of edge costs  $H_e : \mathbb{T}^n \rightarrow \mathbb{R}$ , for  $e \in \mathcal{E}$ . Then it is easy to see that the optimization problem

$$(1.4) \quad \begin{aligned} \min \quad & \mathcal{H}(\theta) = \sum_{(i,j) \in \mathcal{E}} H_e(\theta_i - \theta_j), \\ \text{subject to:} \quad & \theta \in \mathbb{T}^n. \end{aligned}$$

gives rise to an elastic network on the  $n$ -torus with elastic energy  $\mathcal{H}$ . The elastic network problem, for the torque vector  $\tau = \mathbb{0}_n$ , is equivalent to finding critical points of the elastic energy function  $\mathcal{H}(\theta)$  satisfying the constraint  $|\theta_i - \theta_j| \leq \gamma$ .

Having introduced flow and elastic networks on the  $n$ -torus, we now elaborate on several research questions that naturally arise for these systems. Given a flow or elastic network on the  $n$ -torus,

$Q_1$ : does a solution exist and, if so, is it unique? Alternatively, how do we enumerate the solutions as a function of all system parameters?

$Q_2$ : how can the solutions be distinguished and localized on the  $n$ -torus?

$Q_3$ : can we design an algorithm that is guaranteed to compute all solutions?

Additionally, in many network problems, the edge variables themselves are at least as interesting as the underlying nodal phases. Indeed, edge variables describe the flows of the commodity and the elastic energy among the network nodes. Therefore, we will consider the following additional questions:

$Q_4$ : how do different solutions lead to different patterns of edge variables?

$Q_5$ : what is the maximum flow or elastic energy in a given edge as a function of network parameters?

**Applications.** We here present three applications of flow and elastic networks on the  $n$ -torus and briefly discuss the importance of questions ( $Q_1$ )-( $Q_5$ ) in their study.

*Active power flow equations.* In the context of AC power grids with constant voltage magnitudes, the active power flow equation for lossless AC circuits is

$$(1.5) \quad p_i = \sum_{j=1}^n Y_{ij} V_i V_j \sin(\theta_i - \theta_j),$$

where  $p_i, V_i, \theta_i$  are active power supply/demand, voltage magnitude and voltage phase at node  $i$ , respectively, and  $Y_{ij}$  is the line susceptance at edge  $(i, j) \in \mathcal{E}$ . In practice, the power transmitted on a power line is limited by thermal constraints. The angular difference  $\theta_i - \theta_j$  is called the power angle of the line  $(i, j)$ , and the line thermal constraints can be expressed as

$$(1.6) \quad |\theta_i - \theta_j| \leq \gamma, \quad \text{for all } (i, j) \in \mathcal{E},$$

for some maximum power angle  $\gamma \in [0, \frac{\pi}{2})$ . Notably, the active power flow equation (1.5) together with the thermal constraints (1.6) are precisely of the form (1.1a)-(1.1c) with  $h_e(y) = \sin(y)$  on each edge  $e$ .

An important feature in AC power grids is the existence of multistable operating points in the network corresponding to solutions of active power flow equation (1.5). It is well-known that the transition between these distinct stable operating points is sometimes accompanied by large, undesirable changes in the circulating power flows [9]. Circulating flows do not deliver usable power to customers, increase power losses and line congestion, and might cause pricing volatility. The Lake Erie loop, which consists of roughly 1000 miles of transmission lines through Ontario and five American states, presents a classic example of the challenge that circulating power flows present to power grid stability [22]. In order to prevent large failures and black-outs caused by the circulant flows, a theoretical understanding of different operating points of the system and their loop flows is essential.

*Collective motion in engineering and biology.* An insightful example of elastic networks on the  $n$ -torus arises in the study of collective motion in biological and engineering networks. Consider a group of  $n$  agents moving with unit speed on a two-dimensional plane with the pairwise communication and sensing patterns between the agents given by the edge set  $\mathcal{E}$ . The motion of each agent  $k$  is described by its position  $r_k = x_k + iy_k \in \mathbb{C} \simeq \mathbb{R}^2$ , its heading angle  $\theta_k \in \mathbb{T}^1$ , and a steering control law  $u_k = u_k(r, \theta)$  depending on the position and heading angles of the other agents in the group. Formally, the motion of agent  $k$  is given by:

$$(1.7) \quad \dot{r}_k = e^{i\theta_k}, \quad \dot{\theta}_k = u_k(r, \theta).$$

For a network of agents described by the model (1.7), a well-studied form of collective motion is *flocking*, whereby particles asymptotically reach consensus on their heading angles. A second important form of collective motion is the so-called *circular motion* (or *vortex motion*). In circular motion, agents exhibit periodic movements around a circle, where their headings are different vertices on the circle [35]. One can define the elastic energy using the so-called [59] *spacing potential* on the  $n$ -torus:

$$(1.8) \quad \mathcal{H}(\theta) = \sum_{(k,j) \in \mathcal{E}} (1 - \cos(\theta_k - \theta_j)).$$

The spacing potential has several critical points and its global maximum and minimum corresponds to the circular motion and flocking, respectively [35]. Using a gradient flow controller  $u_k = \omega_0 - \frac{\partial \mathcal{H}(\theta)}{\partial \theta_k}$  which depends on a scalar  $\omega_0 \in \mathbb{R}$ , the network of

particles (1.7) can be considered an elastic network on the  $n$ -torus where the elastic energy at each edge  $(k, j)$  is given by  $1 - \cos(\theta_k - \theta_j)$ . In engineering networks, the energy function approach can be used to design more complicated patterns of collective motion. The idea is to utilize appropriate stabilizing control laws to steer the system to desired critical points of the energy function [35]. However, existence of other stable critical points for the energy function and their locations have a large effect on transient and steady-state behavior of the closed-loop system. This motivates a comprehensive study of the critical points of various energy functions on the  $n$ -torus.

*Coupled oscillators and associative memory networks.* Synchronization in networks of coupled oscillators is an emerging phenomenon with important applications in biology, physics, and engineering. The celebrated Kuramoto model is one of the simplest coupled-oscillator model exhibiting synchronization. In this model, each oscillator has a phase  $\theta_i \in \mathbb{T}^1$  and a natural frequency  $\omega_i \in \mathbb{R}$ ; the interactions between oscillators are described by a weighted undirected graph  $G$ , whose edge weights  $a_{ij}$  denote the coupling strength between oscillators  $i$  and  $j$ . The dynamics of the  $i$ th oscillator is given by:

$$(1.9) \quad \dot{\theta}_i = \omega_i - \sum_{j=1}^n a_{ij} \sin(\theta_i - \theta_j)$$

Simple calculations show that (i) synchronous trajectories (i.e., trajectories with identical frequencies) of the Kuramoto model are precisely solutions to a flow network problem (1.1a)-(1.1b) with sinusoidal flow functions and that (ii) solutions satisfying the constraint (1.1c) for  $\gamma < \pi/2$  are locally exponentially stable [14, Lemma 2]. One of the applications of coupled oscillators is associative memory networks. Associative memory is a type of content-addressable memory for recognizing special patterns using partial information. In [24], Hopfield proposed to consider patterns of memory as dynamically stable attractors. Motivated by this idea, the Kuramoto model and its generalizations together with a Hebb's learning rule for the couplings have been used to design associative memory networks [25, 57]. In these networks, binary patterns of memory are encoded as stable frequency-synchronized solutions of the coupled oscillator network [25, 57]. For these models of associative memory, the performance is measured by the number and the size of basin of attraction of stable frequency-synchronized states [57]. Therefore, to study the performance of these associative memory networks, it is essential to develop a theoretical framework for computing the stable frequency synchronized solutions of coupled-oscillator networks.

**Relevant literature.** Numerous research works have studied the multiplicity of solutions of networks on the  $n$ -torus and its connections with the structural properties of the network. In the physics community, much effort has focused on studying the equilibrium points for the Kuramoto coupled-oscillator model and its generalizations. To our knowledge, [16] is the first paper that studies existence of multi-stable equilibria in a ring of Kuramoto oscillators. The phenomenon of multistability has been further explored in the generalized Kuramoto model with small world graph [42] and with Cayley graphs [44]. An algorithm for computing the multi-stable equilibria of ring network of coupled oscillators is proposed by [62]. For Kuramoto coupled oscillators with zero natural frequencies, the uniqueness of the zero stable equilibrium point for dense graph has been studied in [68, 37]. The region of attraction of multistable equilibrium points on a  $k$ -nearest neighbor graphs is studied in [74]. For Kuramoto model with second order couplings, [57] studies the stability and basin of attraction



of equilibrium points. In [40], the notion of winding vector for an arbitrary graph is introduced as the sum of the phase differences along a cycle basis. Moreover, it is shown that for a planar graph, there is a one-to-one correspondence between the winding vectors and the equilibrium points of the Kuramoto model with phase differences less than  $\pi/2$  [40, Lemma 3]. The analysis in [40] also provides upper and lower bounds on the number of stable equilibrium points of Kuramoto coupled oscillators with planar topology. [3] uses Morse Theory to provide an upper bound on the number of stable equilibrium points of the Kuramoto model. [17] provide an asymptotic estimate on the number of equilibrium points of the Kuramoto model by identifying the equilibrium points with suitable lattice points. Numerical algorithms based on homotopy continuation and algebraic geometry have been developed in [46, 10] to compute the equilibrium points of the Kuramoto model.

In the power system community, multiplicity of solutions to active power flow equations has been studied intensively. [31] is the first paper to rigorously study multistable solutions of the active power flow equation and their associated loop flows. Several papers [9, 12, 29] have investigated mechanisms that create large loop flows and have shown that loop flows persist even when the network returns to its normal operating condition. In [9], the basins of attraction for loop flows has been studied using Lyapunov theory. The papers [9, 12, 29] acknowledge the connection between loop flows and winding numbers of the cycles in the graph. The holomorphic embedding load-flow method (HELM) is proposed in [70] to find all solutions of power flow equations. Although HELM is guaranteed to find the operable solution of the power flow equations, it is reported to be much slower than the Newton–Raphson methods [61]. In [39], an algorithm based on a topological continuation argument is developed to solve the power flow problem. However, a counterexample for this method using a five-bus system has been constructed in [52]. This continuation method is revisited and modified in [36]. Techniques for solving the optimal power flow problem (OPF) can also be used to solve the power flow problem. OPF problems have been studied extensively in the power network literature, e.g., see [53, 54, 51]. Unfortunately, due to the non-convex nature of the OPFs, these algorithms are not guaranteed to compute feasible solutions for arbitrary topologies [38].

**Contributions.** This paper provides a rigorous graph-theoretic and geometric framework to analyze the solutions of flow and elastic network problems on the  $n$ -torus. Our framework provides comprehensive answers to questions  $(Q_2)$  and  $(Q_3)$ , and it provides novel insights into questions  $(Q_1)$ ,  $(Q_4)$ , and  $(Q_5)$ . Specifically, this paper provides the following four main contributions:

- (i) We introduce a unifying formalism to study network problems on the  $n$ -torus.
- (ii) We present a novel partition of the  $n$ -torus, called the *winding partition*, induced by cycles in the underlying graph.
- (iii) We prove that each winding cell contains at most a unique solution of the flow network problem and elastic network problem.
- (iv) We present a complete search algorithm, which finds every solution to the flow and elastic network problems on a suitable subset of the  $n$ -torus.

We next discuss these contributions in detail.

In this paper, we formally introduce flow and elastic networks on the  $n$ -torus, and we state the problem of finding all solutions of these networks. While these problems have been studied in various disciplines, we provide a novel, unifying framework to formalize them. We review several applications of flow and elastic network problems on the  $n$ -torus. In Section 2, we show that, by establishing a suitable correspondence

between the supply/demand vectors and the torque vectors and between the flow functions and the elastic energy functions, the solutions of flow network problems and elastic network problems coincide.

In Section 3, we provide a novel algebraic graph theory on the  $n$ -torus. We establish a fundamental property of angle differences around cycles in graphs, which amounts to a *Kirchhoff's angle law*, generalization of the classic voltage law. We introduce the notion of winding vector as a map from the  $n$ -torus to a discrete set and thereby define a novel partition of the  $n$ -torus into *winding cells*.

In Section 4, we focus on flow network problems with monotone flow functions over suitable domains. We show that, in each winding cell, there exists at most one solution for the flow network problem. This “at-most uniqueness” result shows that winding cells can be used to localize the multiple solutions of the flow network problem, thereby providing a graph-theoretic and geometric answer to question (Q<sub>2</sub>). This result also shows that the winding partition is a key geometric concept to study the flow network problem. Finally, this result allows us to upper bound the number of solutions to the flow network problem (on an arbitrary graph), partially answering question (Q<sub>1</sub>). The rest of Section 4 addresses question (Q<sub>4</sub>) by examining “circulating” or “loop” flows around cycles in the network. We establish a bijection between a solution’s winding vector and the circulating flow associated with that solution for flow networks with arbitrary topology and arbitrary monotone flow functions. It is worth mentioning that this bijection has been studied in the literature for Kuramoto coupled-oscillator networks with the ring topology in [12] and with the planar topology in [40]. We show that, in a flow network with strictly increasing flow functions and a single cycle, the circulating flow around the cycle increases monotonically with respect to the winding number.

In Section 5, we recast the flow and elastic network problems as a system of equations with explicit dependence on the winding vector of the solution. Unlike the flow network problem, this new formulation has at most one solution. We propose an iterative algorithm, called the *projection iteration*, that exploits these equations to either solve the problem in a given winding cell, or determine that no such solution exists. Using this iteration, we propose a complete search algorithm to find all solutions of flow and elastic network problems on the  $n$ -torus, as stated in question (Q<sub>3</sub>). In Section 5.3, we provide a comprehensive analysis of the computational complexity of each component of this algorithm. The power systems literature contains many algorithms to find these solutions in the context of active power flow solvers; however, convergence is only guaranteed for some special graphs, whereas our algorithm provably converges on arbitrary topologies.

Finally, in Section 6, we present numerical experiments on special cases of the active power flow equations. We consider two different test cases: a 12-node ring and the IEEE RTS 24 testcase. First, we introduce a notion of transmission capacity and a notion of network congestion. We utilize the projection iteration to numerically study the capacity and congestion in a 12-node ring power grid under two different power profiles. Our numerical analysis shows that, under certain cases, an increase in loop flow can lead to an increase in the network’s power transmission capacity. For the IEEE RTS 24 testcase, we modify the power supply/demand vector and find a solution for the active power flow equations with non-zero winding vector. Moreover, we compare the time efficiency of the projection iteration against the Newton–Raphson method for computing the solutions of the active power flow equations. The numerical analysis in this section sheds some light on question (Q<sub>5</sub>); however, a more comprehensive answer is still the subject of future research.



**2. Preliminary concepts and results.** We start this section by introducing the notation that are essential for our framework in this paper.

**2.1. Notation and mathematical conventions.** Let  $\mathbb{R}$  and  $\mathbb{C}$  denote the set of real and complex numbers, respectively. For every  $x \in \mathbb{R}^n$  and every  $r > 0$ , we define the open disk  $D_\infty(\mathbf{x}, r)$  by

$$D_\infty(\mathbf{x}, r) = \{\mathbf{y} \in \mathbb{R}^n \mid \|\mathbf{y} - \mathbf{x}\|_\infty < r\}.$$

For an interval  $I \subseteq \mathbb{R}$ , the scalar function  $f : I \rightarrow \mathbb{R}$  is monotone on  $I$ , if it is either strictly increasing or strictly decreasing on  $I$ . For a matrix  $A \in \mathbb{R}^{n \times m}$ , the image of  $A$  is denoted by  $\text{Img}(A)$  and the kernel of  $A$  is denoted by  $\text{Ker}(A)$ . For a positive-definite diagonal matrix  $D \in \mathbb{R}^{n \times n}$ , the  $D$ -weighted vector-norm is

$$\|v\|_D = \|D^{\frac{1}{2}}v\|_2, \quad \text{for all } v \in \mathbb{R}^n,$$

and the induced  $D$ -weighted matrix-norm is

$$\|X\|_D = \|D^{\frac{1}{2}}XD^{-\frac{1}{2}}\|_2, \quad \text{for all } X \in \mathbb{R}^{n \times n}.$$

**Algebraic graph theory.** Let  $G$  denote an undirected graph with nodes  $\{1, \dots, n\}$  and edge set  $\mathcal{E}$  with cardinality  $m$ . Given an arbitrary orientation and ordering of the edges, let  $B$  denote the corresponding incidence matrix defined component-wise as  $B_{kl} = 1$  if node  $k$  is the sink node of edge  $l$  and as  $B_{kl} = -1$  if node  $k$  is the source node of edge  $l$ ; all other elements are zero [19, § 8.3]. If  $x \in \mathbb{R}^n$  is a nodal variable (with  $x_i$  associated to the  $i$ th node), then the flow vector associated to  $x$  is the edge variable  $B^\top x \in \mathbb{R}^m$  (with  $(B^\top x)_e = x_i - x_j$  associated to the oriented edge  $e = (i, j)$ ). A *cycle* in  $G$  is an ordered sequence of three or more nodes such that there is an edge between every two consecutive nodes, the first and last nodes are the same, and no other node is repeated. An undirected graph  $G$  is *cyclic* if it contains at least one cycle.

For each cycle  $\sigma$  in  $G$ , the length of  $\sigma$  is denoted by  $n_\sigma$  and the *signed cycle vector*  $v_\sigma \in \{-1, 0, 1\}^m$  is composed of entries

$$(v_\sigma)_e = \begin{cases} +1, & \text{if the edge } e \text{ is traversed positively by } \sigma, \\ -1, & \text{if the edge } e \text{ is traversed negatively by } \sigma, \\ 0, & \text{otherwise.} \end{cases}$$

for each  $e \in \mathcal{E}$  [19, § 14.2]. The *cycle space* of  $G$  is the subspace of  $\mathbb{R}^m$  spanned by the signed cycle vectors of all cycles in  $G$ ; equivalently, the cycle space is  $\text{Ker}(B)$  [19, § 14.2]. A set of cycles  $\Sigma = \{\sigma_1, \dots, \sigma_{m-n+1}\}$  is a *cycle basis* for  $G$  if the corresponding set of signed cycle vectors  $\{v_{\sigma_1}, \dots, v_{\sigma_{m-n+1}}\}$  is a basis for the cycle space. If  $\Sigma = \{\sigma_1, \dots, \sigma_{m-n+1}\}$  is a cycle basis for  $G$ , then the length of  $\Sigma$  is  $\sum_{i=1}^{m-n+1} n_{\sigma_i}$ . A cycle basis with minimal length is called a *minimum cycle basis*.

Note that many authors in the graph theory literature use similar but *discrete* definitions of cycle space and cycle basis. In [27, 30], for example, a “cycle” is a subgraph where every vertex has even degree, and a “cycle basis” is a set of “cycles” that can generate any “cycle” by the logical XOR operation, so the “cycle space” is a vector space on the field  $\text{GF}(2)$  (instead of  $\mathbb{R}$ ). Fortunately, a straightforward consequence of [30, Lemma 2.4] is that the signed cycle vectors corresponding to these discrete basis “cycles” are also a basis for  $\text{Ker}(B)$ . Therefore, we can rely on this literature in future sections for the computation of cycle bases.

Given a connected undirected graph  $G$  with cycle basis  $\Sigma = \{\sigma_1, \dots, \sigma_{m-n+1}\}$ , the *cycle-edge matrix* is

$$(2.1) \quad C_\Sigma = \begin{bmatrix} v_{\sigma_1}^\top \\ \vdots \\ v_{\sigma_{m-n+1}}^\top \end{bmatrix} \in \mathbb{R}^{(m-n+1) \times m}.$$

We refer to Lemma A.1 for additional properties of the cycle-edge matrix. Figure 3 shows some polygonal graphs with oriented edges and cycle bases.

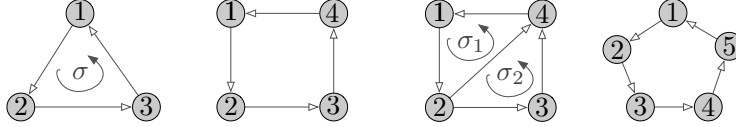


Fig. 3: The triangle, the square, the square-with-diagonal, and the pentagon graph. The triangle and the square-with-diagonal graphs are drawn with a cycle basis.

Next, assume each edge  $(i, j)$  has a weight  $a_{ij}$  and define the diagonal edge weight matrix  $\mathcal{A} = \text{diag}(a_{ij}) \in \mathbb{R}^{m \times m}$ . The Laplacian matrix of  $G$  is  $L = B\mathcal{A}B^\top$ . Recall that  $L$  is singular and its Moore–Penrose pseudoinverse  $L^\dagger$  has the following properties:  $LL^\dagger L = L$ ,  $L^\dagger LL^\dagger = L^\dagger$ ,  $L^\dagger L = (L^\dagger L)^\top$ , and  $LL^\dagger = (LL^\dagger)^\top$ . For a positive definite diagonal matrix  $D \in \mathbb{R}^{m \times m}$ , the  $D$ -weighted cycle projection matrix  $\mathcal{P}_D$  is the oblique projection onto  $\text{Ker}(B)$  parallel to  $\text{Img}(DAB^\top)$  given by

$$(2.2) \quad \mathcal{P}_D = I_m - DAB^\top(BDAB^\top)^\dagger B.$$

If  $G$  is connected, then the  $D$ -weighted cycle projection matrix  $\mathcal{P}_D$  is idempotent and its eigenvalues are 0 and 1 with algebraic (and geometric) multiplicity  $n - 1$  and  $m - n + 1$ , respectively. Moreover, one can show that  $\text{Ker}(\mathcal{P}_D D\mathcal{A}) = \text{Img}(B^\top)$ . We refer to Lemma A.2 for the proof of these properties. Additional properties of this projection are in [28, Theorem 5].

**The  $n$ -torus.** Let  $\mathbb{T}^1$  be the unit circle with its standard Riemannian structure. Given angles  $\alpha, \beta \in \mathbb{T}^1$ , the geodesic distance between  $\alpha$  and  $\beta$ , denoted by  $|\alpha - \beta|$ , is the length of the shortest arc in  $\mathbb{T}^1$  connecting  $\alpha$  to  $\beta$ . The *counterclockwise difference* on  $\mathbb{T}^1$  is the map  $d_{cc} : \mathbb{T}^1 \times \mathbb{T}^1 \rightarrow [-\pi, \pi)$  defined by:

$$d_{cc}(\alpha, \beta) = \begin{cases} |\alpha - \beta|, & \text{if the counterclockwise arc from } \alpha \text{ to } \beta \text{ is shorter than } \pi, \\ -|\alpha - \beta|, & \text{otherwise.} \end{cases}$$

If we identify  $\mathbb{T}^1 \simeq [-\pi, \pi)$ , for every  $\alpha, \beta \in [-\pi, \pi)$ , the counterclockwise difference  $d_{cc}(\alpha, \beta)$  is given by  $d_{cc}(\alpha, \beta) = \text{mod}((\beta - \alpha), 2\pi) - \pi$ . Let  $G$  denote an undirected graph with nodes  $\{1, \dots, n\}$  and edge set  $\mathcal{E}$  with cardinality  $m$ . Given an arbitrary orientation and ordering of the edges, let  $B$  denote the corresponding incidence matrix. If  $\theta \in \mathbb{T}^n$  (with  $\theta_i$  associated to the  $i$ th node of  $G$ ), then, by abuse of notation, we write  $\theta_i - \theta_j$  to refer to  $d_{cc}(\theta_i, \theta_j)$  and we write  $(B^\top \theta)$  to refer to the vector in  $\mathbb{R}^m$  defined by

$$(2.3) \quad (B^\top \theta)_e := \theta_i - \theta_j = d_{cc}(\theta_i, \theta_j), \quad \text{for every } e = (i, j) \in \mathcal{E}.$$

The *punctured  $n$ -torus*  $\mathbb{T}_0^n$  is

$$\mathbb{T}_0^n = \{\theta \in \mathbb{T}^n \mid |\theta_i - \theta_j| < \pi \text{ for each } (i, j) \text{ edge of } G\}.$$

Note that  $\text{closure}(\mathbb{T}_0^n) = \mathbb{T}^n$ . We also need the notion of quotient space. For every angle  $s \in \mathbb{T}^1 \simeq [-\pi, \pi)$ , define the rotation operator  $\text{rot}_s : \mathbb{T}^n \rightarrow \mathbb{T}^n$  by  $\text{rot}_s(\theta) = (\theta_1 + s, \dots, \theta_n + s)^\top$ . Using this rotation operator as a group action, we define the *reduced  $n$ -torus* as the quotient space  $\mathbb{T}^n/\mathbb{T}^1$  and the *reduced punctured  $n$ -torus* as the quotient space  $\mathbb{T}_0^n/\mathbb{T}^1$ . For every  $\theta \in \mathbb{T}^n$ , the equivalent class of  $\theta$  in the reduced  $n$ -torus  $\mathbb{T}^n/\mathbb{T}^1$  is denoted by  $[\theta]$ .

## 2.2. Equivalence of flow and elastic network problems on the $n$ -torus.

Having introduced the flow network problem 1 and the elastic network problem 2 on the  $n$ -torus, we investigate the connection between their solutions. Adopting the analogy that (i) supply/demand vectors are torque vectors, and (ii) flow functions are the derivatives of elastic energy functions, the next result establishes a one-to-one correspondence between the solutions of flow networks and elastic networks.

**THEOREM 2.1** (Equivalence of network problems on the  $n$ -torus). *Let  $G$  be a undirected graph,  $q \in \mathbb{1}_n^\perp$  be a balanced vector,  $\gamma \in [0, \pi)$  be a phase angle,  $\{h_e\}_{e \in \mathcal{E}}$  be a family of continuously differentiable  $2\pi$ -periodic odd functions, and  $\{H_e\}_{e \in \mathcal{E}}$  be a family of twice differentiable  $2\pi$ -periodic even functions such that, for each edge  $e$  and each angle  $\alpha \in (-\gamma, \gamma)$ ,*

$$H_e(\alpha) - H_e(0) = \int_0^\alpha h_e(\beta) d\beta \quad \Longleftrightarrow \quad \frac{dH_e}{d\alpha}(\alpha) = h_e(\alpha).$$

*Then, for  $\theta \in \mathbb{T}^n$ , the following statements are equivalent:*

- (i) *there exists  $f \in \mathbb{R}^m$  such that  $(f, \theta)$  solves the flow network problem (1.1) for  $(G, \{h_e\}_{e \in \mathcal{E}}, q, \gamma)$ ;*
- (ii)  *$\theta$  solves the elastic network problem (1.3) for  $(G, \{H_e\}_{e \in \mathcal{E}}, q, \gamma)$ .*

Theorem 2.1 guarantees that any result about the flow network setting is directly applicable to the elastic network setting and vice versa. For the rest of this paper, we focus on flow network problems on the  $n$ -torus.

**2.3. Acyclic flow network problems on the  $n$ -torus.** In this part, we study the flow network problem (1.1) over connected and acyclic graphs. It turns out that, for acyclic networks, the solvability of the flow network problem (1.1) on the  $n$ -torus can be completely characterized using a simple algebraic inequality. Moreover, one can find a closed-form formula for the flows.

**THEOREM 2.2** (Acyclic flow network problem on the  $n$ -torus). *Consider the flow network problem (1.1) for  $(G, \{h_e\}_{e \in \mathcal{E}}, p_{\text{sd}}, \gamma)$  and suppose that  $G$  is a connected and acyclic graph and each function  $h_e$ ,  $e \in \mathcal{E}$  is monotone on the interval  $[-\gamma, \gamma]$ . Then the following statements are equivalent:*

- (i)  *$|(B^\top L^\dagger p_{\text{sd}})_e| \leq |h_e(\gamma)|$ , for all  $e \in \mathcal{E}$ ,*
- (ii) *there exists a unique solution  $(f^*, \theta^*)$  for the problem (1.1) on the  $n$ -torus.*

*Moreover, if any of the equivalent conditions (i) or (ii) holds, then  $f^* = AB^\top L^\dagger p_{\text{sd}}$ .*

Compared to the literature, Theorem 2.2 extends [14, Theorem 2] and [40, Corollary 2] to the flow networks on the  $n$ -torus with arbitrary monotone flow functions. Theorem 2.2 highlights the role of the network's cycle structure in multiplicity of solutions of the flow network problem (1.1) on the  $n$ -torus. In the rest of this paper, we assume that the graph  $G$  is connected (without loss of generality) and cyclic.

**3. Algebraic graph theory on the  $n$ -torus.** Algebraic graph theory provides a widely established framework to study  $\mathbb{R}$ -valued functions on graphs using linear algebraic structures [5]. In this section, we generalize classical concepts from algebraic graph theory to the setting where the graph nodal variables take value on the circle  $\mathbb{T}^1$ . The starting idea is to extend the classic Kirchhoff's voltage law (KVL) to  $\mathbb{T}^1$ -valued functions on the graph. For  $\mathbb{R}$ -valued functions, KVL states that the sum of nodal differences along each simple cycle is zero. Remarkably,  $\mathbb{T}^1$ -valued functions on a graph exhibit richer behavior. For such functions, one can associate an integer, called the winding number, to each simple cycle and show that the sum of angular differences along the cycle is equal to its winding number. Loosely speaking, the winding number of a cycle counts the number of turns (in counterclockwise direction) of the  $\mathbb{T}^1$ -valued function along the cycle. We start our treatment by introducing the notion of winding number.

**DEFINITION 3.1** (Winding number, vector, and map). *Let  $G$  be a cyclic connected undirected graph and  $\theta \in \mathbb{T}_0^n$ . Then*

(i) *for every cycle  $\sigma$  in  $G$  with  $n_\sigma$  nodes, the winding number of  $\theta$  along  $\sigma$  is*

$$w_\sigma(\theta) = \frac{1}{2\pi} \sum_{i=1}^{n_\sigma} d_{cc}(\theta_i, \theta_{i+1}),$$

*where we assume  $\sigma = (1, \dots, n_\sigma, 1)$  without loss of generality and  $\theta_{n_\sigma+1} = \theta_1$  by convention;*

(ii) *for every cycle basis  $\Sigma = \{\sigma_1, \dots, \sigma_{m-n+1}\}$  in  $G$ , the winding vector of  $\theta$  along the basis  $\Sigma$  is the vector*

$$[w_{\sigma_1}(\theta), \dots, w_{\sigma_{m-n+1}}(\theta)]^\top;$$

(iii) *for every cycle basis  $\Sigma = \{\sigma_1, \dots, \sigma_{m-n+1}\}$  in  $G$ , the winding map  $\mathbf{w}_\Sigma : \mathbb{T}_0^n \rightarrow \mathbb{Z}^{m-n+1}$  along the basis  $\Sigma$  is*

$$\mathbf{w}_\Sigma(\theta) = [w_{\sigma_1}(\theta), \dots, w_{\sigma_{m-n+1}}(\theta)]^\top.$$

The notion of winding number is a classical concept in mathematics and its rigorous definition dates back to the early work of Alexander [2]. In differential topology, the notions of *index of a smooth vector field* and *degree of a continuous map* can be considered as generalizations of the winding number [23]. To the best of our knowledge, [74] is the first work that introduces the notion of winding number to characterize the fixed points of a coupled oscillator network. The connection between the number of fixed points of the Kuramoto model and the winding number of the solution has been first explored in [58] for ring graphs. More recently, the notions of winding number and winding vector have been used in [40] and [12] to study multistability in networks of Kuramoto oscillators.

The winding number, winding vector, and winding map are invariant under the rotation operator  $\text{rot}_s$ , for  $s \in [-\pi, \pi)$ , that is, every cycle  $\sigma$  and every  $\theta \in \mathbb{T}_0^n$  satisfy  $w_\sigma(\theta) = w_\sigma(\text{rot}_s(\theta))$ . Therefore the winding number, winding vector, and winding map are well-defined on the reduced punctured  $n$ -torus  $\mathbb{T}_0^n/\mathbb{T}^1$ . The winding vector of  $\theta$  along the basis  $\Sigma$  collects in one quantity all the information required to compute the winding number of each cycle of the graph. The winding number, vector and map  $\mathbf{w}_\Sigma$  and its image  $\text{Img}(\mathbf{w}_\Sigma)$  depend on the cycle basis  $\Sigma$  chosen for  $G$ . However, one can define a basis-independent winding map on  $\mathbb{T}_0^n$  (see Appendix B).

REMARK 3.2 (Algorithms for computing cycle basis). *Several algorithms exist in the literature for computing the cycle basis of an undirected graph. A simple approach is based on finding a spanning tree for  $G$  and runs in  $\mathcal{O}(mc)$  time, where  $c$  is the length of the largest cycle in the graph. To find a cycle basis with the desired extremum properties, one can use the greedy algorithm over the set of all cycles in the graph. However, for many graph families, the number of cycles grows exponentially with the number of nodes (for instance the number of cycles in the complete graph with  $n$  nodes is  $\sum_{k=3}^n \frac{1}{2}(k-1)!\binom{n}{k}$  which grows exponentially with  $n$ ). Therefore, the run time of the greedy algorithm can grow exponentially with the number of nodes  $n$ . To find the minimum cycle basis of undirected unweighted graphs, Horton [27] provided the first-known polynomial-time algorithm; Horton's algorithm runs in  $\mathcal{O}(m^3n)$  time or, in its improvement proposed in [45], in  $\mathcal{O}(m^2n/\log(n) + n^2m)$ . Finally, [15] proposes an algorithm to construct a cycle basis of length  $\mathcal{O}(m\log(n)\log\log(n))$  for unweighted graphs. We refer to [30] for a survey on algorithms and computational complexity of computing minimum cycle bases.*

To illustrate the notion of winding number we consider the triangle graph with cycle  $\sigma = (1, 2, 3, 1)$  in Figure 3. Since the cycle space of the triangle graph is spanned by  $\sigma$ , the winding map with respect to  $\sigma$  is  $\mathbf{w}_\Sigma(\theta) = w_\sigma(\theta)$ . One can show that, if the angles  $(\theta_1, \theta_2, \theta_3) \in \mathbb{T}_0^3$  are contained in an arc of length less than or equal to  $\pi$ , then  $w_\sigma(\theta) = 0$  and, otherwise,  $w_\sigma(\theta) \in \{-1, +1\}$ ; see Figure 4. For example, for

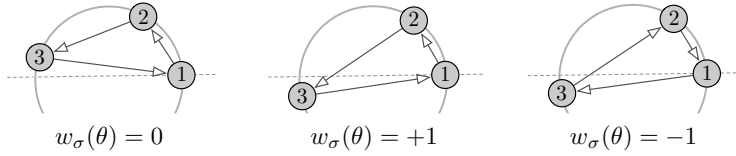


Fig. 4: For the triangle graph, if the angles are strictly contained in an half circle, the winding number is zero. Otherwise, the winding number is  $\pm 1$  depending upon the node numbering and edge orientations.

$\phi = (0, \frac{\pi}{3}, \frac{2\pi}{3})^\top$  and  $\psi = (0, \frac{2\pi}{3}, \frac{4\pi}{3})^\top$ , simple book-keeping shows

$$w_\sigma(\phi) = \frac{1}{2\pi}(\frac{\pi}{3} + \frac{\pi}{3} - \frac{2\pi}{3}) = 0, \text{ and } w_\sigma(\psi) = \frac{1}{2\pi}(\frac{2\pi}{3} + \frac{2\pi}{3} + \frac{2\pi}{3}) = 1.$$

Now, we prove some useful properties for the winding number and winding vectors.

THEOREM 3.3 (Kirchhoff's angle law). *Let  $G$  be a cyclic connected undirected graph with  $n$  nodes, and  $m$  edges. Let  $\sigma$  be a cycle on  $G$  with  $n_\sigma$  nodes and  $\Sigma = \{\sigma_1, \dots, \sigma_{m-n+1}\}$  be a cycle basis for  $G$ . Let  $\theta \in \mathbb{T}_0^n$ . Then*

- (i) *the winding number  $w_\sigma(\theta)$  is an integer and  $|w_\sigma(\theta)| \leq \left\lceil \frac{n_\sigma}{2} \right\rceil - 1$ ;*
- (ii) *the winding map  $\mathbf{w}_\Sigma$  is piecewise constant and*

$$|\text{Img}(\mathbf{w}_\Sigma)| \leq \prod_{i=1}^{m-n+1} \left( 2 \left\lceil \frac{n_{\sigma_i}}{2} \right\rceil - 1 \right).$$

Theorem 3.3(i) generalizes the classic Kirchhoff's voltage law (KVL) to the setting of graphs with nodal variables in  $\mathbb{T}^1$ : the sum of the nodal differences along every simple cycle is equal to  $2\pi w$ , where  $w \in \mathbb{Z}$  is the winding number of the cycle.

In order to illustrate the Kirchhoff's angle law and various properties in Theorem 3.3, we get back to the polygonal graphs in Figure 3. We consider the square graph with a diagonal edge and define its cycles  $\sigma_1 = (1, 2, 4, 1)$ ,  $\sigma_2 = (2, 3, 4, 2)$ , and  $\sigma_3 = (1, 2, 3, 4, 1)$ , as in Figure 3. Note that only two cycles are independent in the sense that the signed cycle vectors satisfy  $v_{\sigma_1} + v_{\sigma_2} = v_{\sigma_3}$  and so the set  $\Sigma = \{v_{\sigma_1}, v_{\sigma_2}\}$  is a basis for cycle space of  $G$ . The winding map of the graph  $G$  with respect to basis  $\Sigma$  is given by  $\mathbf{w}_\Sigma(\theta) = [w_{\sigma_1} \ w_{\sigma_2}]^\top$ . Theorem 3.3(i) implies that  $|w_{\sigma_i}(\theta)| \leq \lceil \frac{3}{2} \rceil - 1 = 1$ , for every  $\theta \in \mathbb{T}_0^4$  and every  $i \in \{1, 2\}$ . Therefore,  $\text{Img}(\mathbf{w}_\Sigma) \subseteq \{-1, 0, +1\}^2$ . Moreover, one can see that the winding vectors  $[1 \ 1]^\top$  and  $[-1 \ -1]^\top$  are not possible for the square graph with a diagonal. This implies that  $\text{Img}(\mathbf{w}_\Sigma) \subset \{-1, 0, +1\}^2$  and therefore, in general, the inequality in Theorem 3.3(ii) can be strict.

Since winding vector is a piecewise constant map, one can partition the  $n$ -torus into the regions where the winding vector assume a fixed integer vector. These regions are called winding cells.

**DEFINITION 3.4** (Winding cell). *Consider the cyclic connected undirected graph  $G$  with cycle basis  $\Sigma$  and winding map  $\mathbf{w}_\Sigma$ . For  $\mathbf{u} \in \text{Img}(\mathbf{w}_\Sigma)$ , the  $\mathbf{u}$ -winding cell is the subset of  $\mathbb{T}_0^n$  defined by*

$$\Omega_{\mathbf{u}}^G = \mathbf{w}_\Sigma^{-1}(\mathbf{u}).$$

For the triangle graph in Figure 3, one can visualize the winding cells. Note that the triangle graph with only cycle  $\sigma = (1, 2, 3, 1)$  has  $\text{Img}(\mathbf{w}_\Sigma) = \{-1, 0, +1\}$ . Therefore, the winding cells of  $\mathbb{T}_0^3$  are

$$\begin{aligned} \Omega_{-1}^G &= \left\{ \theta = (\theta_1, \theta_2, \theta_3)^\top \in \mathbb{T}_0^3 \mid \sum_{i=1}^3 d_{cc}(\theta_i, \theta_{i+1}) = -2\pi \right\}, \\ \Omega_0^G &= \left\{ \theta = (\theta_1, \theta_2, \theta_3)^\top \in \mathbb{T}_0^3 \mid \text{there exists an arc of length } \pi \text{ containing } \theta_1, \theta_2, \theta_3 \right\}, \\ \Omega_1^G &= \left\{ \theta = (\theta_1, \theta_2, \theta_3)^\top \in \mathbb{T}_0^3 \mid \sum_{i=1}^3 d_{cc}(\theta_i, \theta_{i+1}) = 2\pi \right\}. \end{aligned}$$

Figure 5 illustrates these winding cells.

We are now ready to state the main result of this section. Since the winding map is piecewise constant and finite valued, it partitions the  $n$ -torus into a finite number of regions. This partition captures the connection between the geometry of the  $n$ -torus and the cycle structure of the network. As we will see later, it also plays a crucial role in localizing the solutions of flow network problems on the  $n$ -torus.

**THEOREM 3.5** (Winding partition of the  $n$ -torus). *Consider the cyclic connected undirected graph  $G$  with cycle basis  $\Sigma$  and winding map  $\mathbf{w}_\Sigma$ . Then the set  $\{\text{closure}(\Omega_{\mathbf{u}}^G) \mid \mathbf{u} \in \text{Img}(\mathbf{w}_\Sigma)\}$  is a partition of  $\mathbb{T}^n$ , called the  $G$ -winding partition of  $\mathbb{T}^n$ , in the sense that*

- (i)  $\mathbb{T}^n = \bigcup_{\mathbf{u} \in \text{Img}(\mathbf{w}_\Sigma)} \text{closure}(\Omega_{\mathbf{u}}^G)$ ;
- (ii) for every  $\mathbf{u}, \mathbf{v} \in \text{Img}(\mathbf{w}_\Sigma)$ ,  $\mathbf{u} \neq \mathbf{v}$  implies  $\Omega_{\mathbf{u}}^G \cap \Omega_{\mathbf{v}}^G = \emptyset$ .

While Definition 3.4 is mathematically rigorous, it does not provide insight into the topological properties of the winding cells. These insights are particularly important for visualization of the winding partition of the  $n$ -torus developed in Theorem 3.5. In the next theorem, we provide a continuous bijection which allows one to visualize the winding cells as convex polytopes in Euclidean spaces. Using this characterization, we show that the winding cells enjoy several useful properties. (Recall the definition of cycle-edge matrix from equation (2.1) and of the vector  $(B^\top \theta)$  from equation (2.3).)



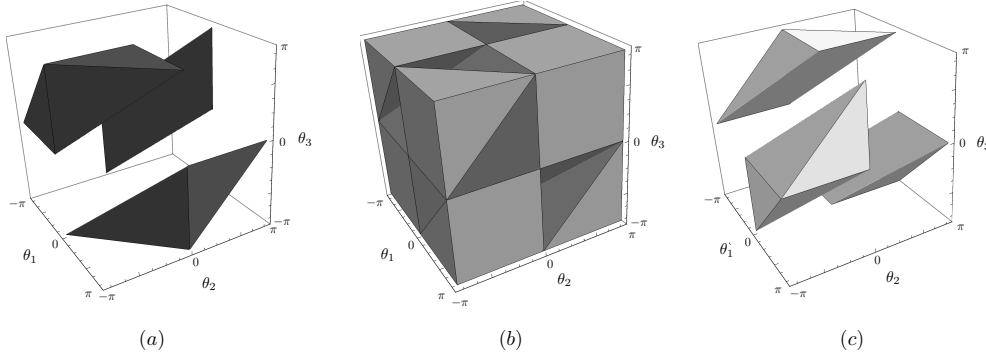


Fig. 5: The winding cells  $\Omega_{-1}^G$ ,  $\Omega_0^G$ , and  $\Omega_1^G$ , induced by the triangle graph on  $\mathbb{T}_0^3$  are shown in Figures (a), (b), and (c), respectively. The three axes are the three angles  $\theta_1, \theta_2, \theta_3$ , each taking values in the interval  $[-\pi, \pi)$ . These axes are periodic on the 3-torus, so all three winding cells are path-connected, despite their disconnected representations in  $\mathbb{R}^3$ .

**THEOREM 3.6** (Polytopic characterization of winding cells). *Consider a connected cyclic undirected graph  $G$  with cycle basis  $\Sigma$ , winding map  $\mathbf{w}_\Sigma$ , and cycle-edge matrix  $C_\Sigma \in \mathbb{R}^{(m-n+1) \times m}$ . Pick  $\mathbf{u} \in \text{Img}(\mathbf{w}_\Sigma)$ . Then*

- (i) *for every  $[\theta] \in \Omega_{\mathbf{u}}^G/\mathbb{T}^1$ , there exists a unique  $\mathbf{x} \in \mathbb{1}_n^\perp$  such that  $(B^\top \theta) = B^\top \mathbf{x} + 2\pi C_\Sigma^\dagger \mathbf{u}$ ;*
- (ii) *define the open convex polytope*

$$P_{\mathbf{u}} = \{\mathbf{x} \in \mathbb{1}_n^\perp \mid \|B^\top \mathbf{x} + 2\pi C_\Sigma^\dagger \mathbf{u}\|_\infty < \pi\}.$$

*Then, the map  $[\theta] \mapsto x$  defined in part (i) is a continuous bijection between the reduced winding cell  $\Omega_{\mathbf{u}}^G/\mathbb{T}^1$  and the polytope  $P_{\mathbf{u}}$ , and it is a homeomorphism on every compact subset of  $\Omega_{\mathbf{u}}^G/\mathbb{T}^1$ .*

In Figure 6(a) and Figure 6(b), we plot the reduced winding cells  $\Omega_{-1}^G/\mathbb{T}^1$ ,  $\Omega_0^G/\mathbb{T}^1$ , and  $\Omega_1^G/\mathbb{T}^1$  induced by the triangle graph and square graph on  $\mathbb{T}_0^3/\mathbb{T}^1$  and  $\mathbb{T}_0^4/\mathbb{T}^1$ , respectively. In Figure 6(c), we plot the reduced winding cells induced by the square-with-diagonal graph (Figure 3) on  $\mathbb{T}_0^4/\mathbb{T}^1$ . The vector on each winding cell indicates its associated winding vector  $\mathbf{w}_\Sigma$ , for  $\Sigma = \{\sigma_1, \sigma_2\}$ . Figure 6 plots the winding cells as functions of counterclockwise distances  $d_{cc}(\theta_i, \theta_{i+1})$  rather than phases  $\theta_i$ , effectively modding out uniform rotations.

We conclude this section by some comments about the role of cycle basis  $\Sigma$  in our framework. First, while the winding map  $\mathbf{w}_\Sigma$  in Definition 3.1 (iii) depends upon  $\Sigma$ , the winding partition of  $\mathbb{T}^n$  in Theorem 3.5 is independent of it, in the sense that, given any other cycle basis  $\Sigma'$ , each winding cell  $\Omega_{\mathbf{u}}^G$ , for  $\mathbf{u} \in \text{Img}(\mathbf{w}_\Sigma)$ , is equal to a cell  $\Omega_{\mathbf{u}'}^G$  for an appropriate  $\mathbf{u}' \in \text{Img}(\mathbf{w}_{\Sigma'})$ . Second, note that the upper bound on the cardinality of  $\text{Img}(\mathbf{w}_\Sigma)$  given in Theorem 3.3(ii) depends upon  $\Sigma$ . While computing the cycle basis that minimizes this upper bound appears computationally complex, it is simple to provide the following approximation. Adopting the shorthand  $|\Sigma| = m - n + 1$ , we compute

$$|\text{Img}(\mathbf{w}_\Sigma)| \leq \prod_{i=1}^{|\Sigma|} \left( 2 \left\lceil \frac{n_{\sigma_i}}{2} \right\rceil - 1 \right) \leq \prod_{i=1}^{|\Sigma|} (n_{\sigma_i} + 1) \leq \left( \frac{\sum_{i=1}^{|\Sigma|} (n_{\sigma_i} + 1)}{|\Sigma|} \right)^{|\Sigma|},$$

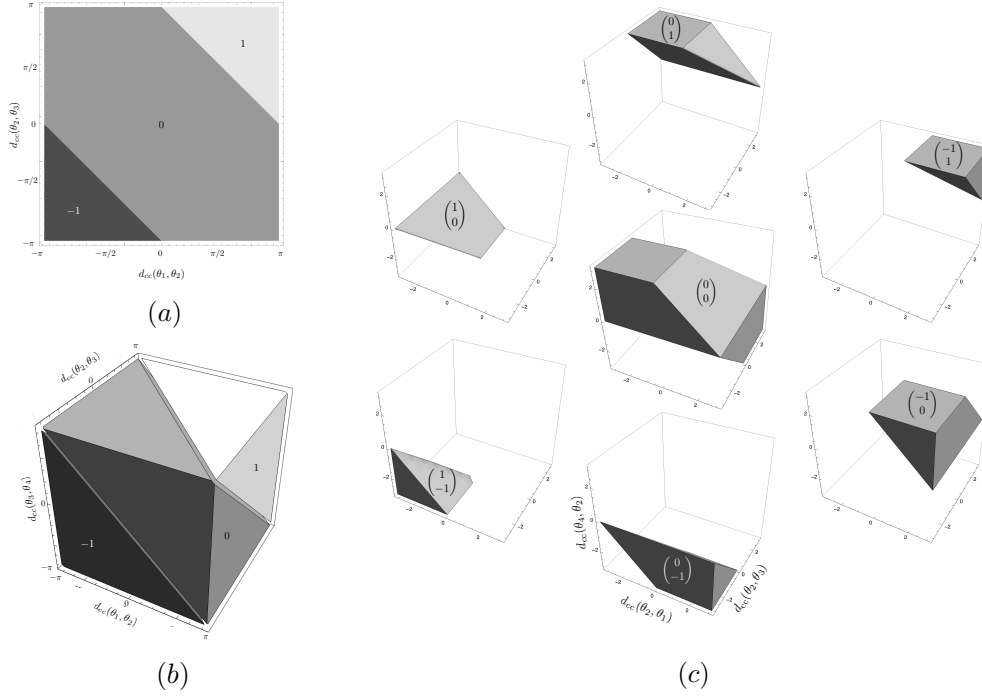


Fig. 6: The reduced winding cells on the triangle graph (a), the square graph (b), and the square-with-diagonal graph (c) on  $\mathbb{T}_0^3/\mathbb{T}^1$ ,  $\mathbb{T}_0^4/\mathbb{T}^1$ , and  $\mathbb{T}_0^4/\mathbb{T}^1$ , respectively. The number (vector) on each region indicates the winding number (winding vector) of that region. In all plots, each axis corresponds to an edge in the graph and indicates the counter-clockwise difference between the incident nodes, on the interval  $[-\pi, \pi)$ .

where we used the inequality of arithmetic and geometric means. Now, the classic result [27, Theorem 6] states that the length of a minimum cycle bases of an unweighted graph is at most  $3(n-1)(n-2)/2$ , so that

$$|\text{Img}(\mathbf{w}_\Sigma)| \leq \left( \frac{3(n-1)(n-2)}{m-n+1} + 1 \right)^{m-n+1}.$$

Alternatively, the length of minimum cycle basis of an unweighted graph is known [15] to be in  $\mathcal{O}(m \log(n) \log(\log(n)))$  so that there exists a constant  $C$  such that

$$|\text{Img}(\mathbf{w}_\Sigma)| \leq (C \log n \log \log n)^{m-n+1}.$$

If the graph admits a basis of cycles with length at most  $n_\sigma$ , then

$$|\text{Img}(\mathbf{w}_\Sigma)| \leq (2\lceil n_\sigma/2 \rceil - 1)^{m-n+1}.$$

For example, the complete graph  $K_n$  has a cycle basis with  $n_\sigma = 3$  and so, given  $m-n+1 = (n-1)(n-2)/2$ , we know  $|\text{Img}(\mathbf{w}_\Sigma)| \leq 3^{(n-1)(n-2)/2}$ . The two-dimensional grid graph  $G_{h,k}$  with  $n = hk$  nodes and  $m = 2hk - h - k$  edges, has a cycle basis with  $n_\sigma = 4$  so that  $|\text{Img}(\mathbf{w}_\Sigma)| \leq 3^{hk-h-k+1}$ .

**4. Localization and decomposition of network flows.** In this section, we use the tools of Section 3 to study flow network problems on the  $n$ -torus. Recall that Theorem 2.1 ensures that any result about the flow network problem is directly applicable to the elastic networks setting.

We first use the winding partition to localize the solutions of the flow network problem (1.1). In particular, we show that if the flow functions are monotone, then flow network problem (1.1) has at most one solution inside each winding cell.

**THEOREM 4.1** (At most uniqueness of solutions). *Consider the flow network problem (1.1) for  $(G, \{h_e\}_{e \in \mathcal{E}}, p_{\text{sd}}, \gamma)$  and suppose that each flow function  $h_e$ ,  $e \in \mathcal{E}$ , is monotone on the interval  $[-\gamma, \gamma]$ . Let  $\Sigma$  be a cycle basis for  $G$ . Then, for any winding vector  $\mathbf{u} \in \text{Img}(\mathbf{w}_\Sigma)$ , there exists at most one solution  $(f, \theta)$  for flow network problem (1.1), such that  $\theta \in \Omega_{\mathbf{u}}^G$ .*

In the context of Kuramoto coupled oscillators (1.9), it is known that, if the network has a planar topology, then the locally stable synchronous trajectories have distinct winding vectors [12, 40]. Theorem 4.1 can be considered as a generalization of these results to flow networks on the  $n$ -torus with arbitrary topology and arbitrary monotone flow functions. For graphs with a cycle basis of given length, the angle constraint (1.1c) can be used to specify the winding cells in which there is no solution for the flow network problem (1.1).

**COROLLARY 4.2** (Upper bound on the number of solutions). *Consider the flow network problem (1.1) for  $(G, \{h_e\}_{e \in \mathcal{E}}, p_{\text{sd}}, \gamma)$ . Suppose that each flow function  $h_e$ ,  $e \in \mathcal{E}$ , is monotone on  $[-\gamma, \gamma]$  and  $G$  has a cycle basis  $\Sigma = \{\sigma_1, \dots, \sigma_{m-n+1}\}$  with maximum cycle length  $k$ . For  $\mathbf{u} \in \text{Img}(\mathbf{w}_\Sigma)$ , the following statements hold:*

- (i) *if  $\|\mathbf{u}\|_\infty \leq \lfloor \frac{k\gamma}{2\pi} \rfloor$ , then problem (1.1) has at most one solution  $(f, \theta)$  with  $\theta \in \Omega_{\mathbf{u}}^G$ ;*
- (ii) *if  $\|\mathbf{u}\|_\infty > \lfloor \frac{k\gamma}{2\pi} \rfloor$ , then problem (1.1) has no solution  $(f, \theta)$  with  $\theta \in \Omega_{\mathbf{u}}^G$ ; and*
- (iii) *Problem (1.1) has at most  $\prod_{i=1}^{m-n+1} \lfloor \frac{n_{\sigma_i}\gamma}{2\pi} \rfloor$  solutions  $(f, \theta) \in \mathbb{R}^m \times \mathbb{T}^n$ .*

For the special case  $\gamma < \pi/2$ , Corollary 4.2 (i) and (ii) applies to the complete graphs, complete bipartite graphs, and two-dimensional grids and shows that the flow network problem has at most one solution, see Figure 7. In the literature, similar upper bounds for the number of stable solutions of the Kuramoto model (1.9) have been obtained for planar networks [40] and for simple cycles [12]. Corollary 4.2(iii) generalizes the results in [40, 12] to provide an upper bound on the number of solutions of flow networks with arbitrary topology and arbitrary monotone flow functions.

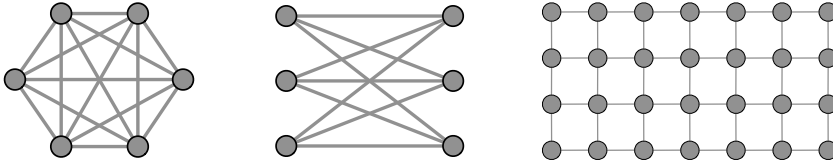


Fig. 7: Corollary 4.2 implies that, the flow network problem (1.1) with  $\gamma < \pi/2$  on complete graphs, complete bipartite graphs, and two-dimensional grid graphs, have at most one solution, independently of supply/demand vector and edge weights.

Next, we propose a natural decomposition for the edge space  $\mathbb{R}^m$  and describe how it relates to the flow network problem (1.1). For every connected undirected

graph  $G$ , the edge space of  $G$  can be uniquely decomposed as follows:

$$(4.1) \quad \mathbb{R}^m = \text{Img}(\mathcal{A}B^\top) \oplus \text{Ker}(B).$$

This oblique decomposition is a special case of the classic orthogonal decomposition into cutset and cycle space, studied in algebraic graph theory, see [5, §2]. Let  $f$  be a flow for the flow network problem (1.1) on the graph  $G$ . For every simple cycle  $\sigma$  in  $G$ , the *loop flow* associated with the cycle  $\sigma$  is the scalar  $v_\sigma^\top f$ , where  $v_\sigma$  is the signed cycle vector associated to the cycle  $\sigma$ .

**THEOREM 4.3** (Decomposition of flows). *Consider the flow network problem (1.1) for  $(G, \{h_e\}_{e \in \mathcal{E}}, p_{\text{sd}}, \gamma)$  and suppose that each flow function  $h_e$ ,  $e \in \mathcal{E}$ , is monotone on the interval  $[-\gamma, \gamma]$ . Let  $\Sigma$  be a cycle basis for  $G$  and suppose that  $(f, \phi), (g, \psi) \in \mathbb{R}^m \times \mathbb{T}^n$  are two solutions for flow network problem (1.1). Then the following statements hold:*

(ii)  $f$  can be decomposed uniquely as

$$f = f^{\text{cut}} + f^{\text{cyc}},$$

where  $f^{\text{cut}} = \mathcal{A}B^\top L^\dagger p_{\text{sd}} \in \text{Img}(\mathcal{A}B^\top)$  is called the cutset flow and  $f^{\text{cyc}} \in \text{Ker}(B)$  is called the cycle flow.

(iii)  $f - g \in \text{Ker}(B)$ , that is, flows differ by a cycle flow;

(iv)  $f = g \iff \mathbf{w}_\Sigma(\phi) = \mathbf{w}_\Sigma(\psi) \iff \phi = \text{rot}_s(\psi)$ , for some  $s \in [-\pi, \pi]$ ;

(v) if  $G$  has exactly one cycle  $\sigma$  and each flow function  $h_e$ ,  $e \in \mathcal{E}$ , is strictly increasing, then

$$w_\sigma(\phi) > w_\sigma(\psi) \iff v_\sigma^\top f > v_\sigma^\top g,$$

that is, loop flows are strictly increasing with respect to winding numbers.

**5. Solving flow network problems on the  $n$ -torus.** In this section, we focus on verifying the existence and computing the solutions of the flow network problem (1.1) on the  $n$ -torus.

One of the classic methods for solving nonlinear equations is the Newton–Raphson method. This method comes with two main disadvantages in the context of the flow network problem (1.1). First, the Newton–Raphson iterations comes with no global convergence guarantee. Therefore, when the iteration does not converge, one cannot infer the lack of solutions. The second issue is the sensitivity of the Newton–Raphson method with respect to initial conditions. This is a critical issue since the flow network problem (1.1) can often have several solutions. Consider for example the flow network problem (1.1) on the 5-torus over the unit-weighted pentagon graph in Figure 3 with flow function  $h_e = \sin$ , for every  $e \in \mathcal{E}$ . For  $p_{\text{sd}} = \mathbb{0}_5$ , the flow network problem has the phase-synchronous solution  $\phi^* = \mathbb{0}_5$  with winding number 0 and the splay-state solution  $\psi^* = (0, \frac{2\pi}{5}, \frac{4\pi}{5}, \frac{6\pi}{5}, \frac{8\pi}{5})^\top$  with winding number +1. Consider the sequence  $\{x^{(n)}\}_{n \in \mathbb{Z}_{\geq 0}}$  generated by the Newton–Raphson algorithm:

$$x^{(n+1)} = x^{(n)} - (BA \text{diag}(\cos(B^\top x^{(n)}))B^\top)^\dagger BA \sin(B^\top x^{(n)}),$$

with initial condition  $x^{(0)} = (0, \frac{\pi}{3}, \frac{\pi}{2}, \frac{2\pi}{3}, 0)^\top$ . While  $\mathbf{w}_\Sigma(x^{(0)}) = 0$ , the Newton–Raphson iterations starting from  $x^{(0)}$  converges to  $\psi^*$  with winding number +1. This example illustrates that the Newton–Raphson method is not consistent with the partition of the  $n$ -torus introduced in Theorem 3.5.

In the previous section, we showed that the winding partition of the  $n$ -torus is useful for localizing the solutions of the flow network problem (1.1). In the following Section 5.1, we provide a novel transcription for problem (1.1) which reveals the role of winding cells. The main advantage of this transcription is to replace the phase angle  $\theta \in \mathbb{T}^n$  (i.e., a continuous variable) with the winding vector  $\mathbf{w}_\Sigma(\theta) \in \mathbb{Z}^{m-n+1}$  (i.e., a discrete variable). Then, in Section 5.2, we introduce an appropriate operator and write this novel transcription as a fixed-point problem. We show that this fixed-point formulation is amenable to analysis using well-known contraction techniques.

**5.1. Winding balance equation.** Using the polytopic characterization of winding cells (3.6), one can identify the counterclockwise angle difference vector ( $B^\top \theta$ ) in the  $\mathbf{u}$ -winding cell with elements in the polytope  $P_{\mathbf{u}}$ . As a result, we get a transcription of the flow network problem (1.1) which reveals the role of the winding partition in this problem. Before we state this winding transcription, for every  $\gamma \in [0, \pi)$ , we introduce the extended flow function  $h_\gamma : \mathbb{R}^m \rightarrow \mathbb{R}^m$ , where, for every  $e \in \{1, \dots, m\}$ , its  $e$ th component is defined by:

$$(h_\gamma)_e(y) = \begin{cases} h_e(y_e), & |y_e| < \gamma, \\ \frac{\partial h_e}{\partial y_e}(\gamma)(y_e - \gamma) + h_e(\gamma), & y_e \geq \gamma, \\ \frac{\partial h_e}{\partial y_e}(\gamma)(y_e + \gamma) + h_e(-\gamma), & y_e \leq -\gamma. \end{cases}$$

Clearly, each function  $(h_\gamma)_e(y)$ ,  $e \in \mathcal{E}$ , depends only on the variable  $y_e$  and it is monotone with respect to  $y_e$ . As a result,  $h_\gamma$  is invertible on  $\mathbb{R}^m$ . Furthermore, define two diagonal matrices  $L_{\min}, L_{\max} \in \mathbb{R}^{m \times m}$  by

$$(L_{\min})_{ee} = \min_{y \in [-\gamma, \gamma]} \frac{\partial h_e(y)}{\partial y} \quad \text{and} \quad (L_{\max})_{ee} = \max_{y \in [-\gamma, \gamma]} \frac{\partial h_e(y)}{\partial y},$$

for all  $e \in \{1, \dots, m\}$ . Since each  $h_e$ ,  $e \in \{1, \dots, m\}$ , is monotone we have  $0 < (L_{\min})_{ee}(L_{\max})_{ee}^{-1} \leq 1$ . This implies that  $\|I_m - L_{\min}L_{\max}^{-1}\|_\infty < 1$ . For every  $\mathbf{u} \in \text{Img}(\mathbf{w}_\Sigma)$ , the  $\mathbf{u}$ -winding balance equation for the flow network problem (1.1) is:

$$(5.1a) \quad Bf = p_{\text{sd}},$$

$$(5.1b) \quad \mathcal{P}_{L_{\min}} L_{\min} \mathcal{A}(h_\gamma^{-1}(\mathcal{A}^{-1}f) - 2\pi C_\Sigma^\dagger \mathbf{u}) = \mathbf{0}_m,$$

$$(5.1c) \quad |f_e| \leq a_{ij}|h_e(\gamma)|, \quad \text{for } e = (i, j) \in \mathcal{E},$$

where  $\mathcal{P}_{L_{\min}}$  is the  $L_{\min}$ -weighted cycle projection matrix. Note that the  $\mathbf{u}$ -winding balance equation has no variable on the  $n$ -torus  $\mathbb{T}^n$ . The following theorem illustrates the connection between solutions of  $\mathbf{u}$ -winding balance equation (5.1) and solutions of the flow network problem (1.1).

**THEOREM 5.1** (Equivalence of  $\mathbf{u}$ -winding balance equation and flow network problem). *Consider the flow network problem (1.1) for  $(G, \{h_e\}_{e \in \mathcal{E}}, p_{\text{sd}}, \gamma)$  and suppose that each flow function  $h_e$ ,  $e \in \mathcal{E}$ , is monotone on  $[-\gamma, \gamma]$ . Let  $\Sigma$  be a cycle basis for  $G$ . Then, for  $\mathbf{u} \in \text{Img}(\mathbf{w}_\Sigma)$  and  $f \in \mathbb{R}^m$ , the following statements are equivalent:*

- (i) *there exists a unique  $\theta \in \Omega_{\mathbf{u}}^G$ , modulo rotations, such that  $(f, \theta)$  is a solution for the flow network problem (1.1); and*
- (ii)  *$f$  is a solution for the  $\mathbf{u}$ -winding balance equation (5.1).*

**5.2. Fixed-point formulation and flow network solver.** The winding transcription (5.1) simplifies the analysis of flow network problem (1.1) on the  $n$ -torus by

reducing the continuous variable  $\theta \in \mathbb{T}^m$  to the finite discrete variable  $\mathbf{w}_\Sigma(\theta)$ . We now provide an equivalent fixed-point formulation for the winding transcription (5.1) which can be analyzed using contraction theory. We first define the space of  $p_{\text{sd}}$ -balanced flows by

$$F_{\text{sd}} = \{f \in \mathbb{R}^m \mid Bf = p_{\text{sd}}\}.$$

To write the  $\mathbf{u}$ -winding balance equation (5.1) as a fixed-point problem, we define the  $\mathbf{u}$ -winding fixed-point map  $T_{\mathbf{u}} : F_{\text{sd}} \rightarrow F_{\text{sd}}$  by:

$$T_{\mathbf{u}}(f) = f - \mathcal{P}_{L_{\min}} L_{\min} \mathcal{A} (h_\gamma^{-1}(\mathcal{A}^{-1} f) - 2\pi C_\Sigma^\dagger \mathbf{u}),$$

where  $\mathcal{P}_{L_{\min}}$  is the  $L_{\min}$ -weighted cycle projection matrix. Using the  $\mathbf{u}$ -winding fixed-point map  $T_{\mathbf{u}}$ , we can write the  $\mathbf{u}$ -winding balance equation (5.1) as the following fixed-point problem:

$$(5.2a) \quad T_{\mathbf{u}}(f) = f,$$

$$(5.2b) \quad |f_e| \leq a_{ij} |h_e(\gamma)|, \quad \text{for } e = (i, j) \in \mathcal{E}.$$

The fixed-point problem (5.2) suggests the definition of the *projection iteration*:

$$(5.3) \quad f^{(k+1)} = T_{\mathbf{u}}(f^{(k)}),$$

$$(5.4) \quad f^{(0)} \in F_{\text{sd}}.$$

for finding solutions of the flow network problem (1.1). The following theorem study the connection between solvability of the flow network problem (1.1) on the  $n$ -torus and the convergence of the projection iteration.

**THEOREM 5.2** (Solvability of flow network problem on the  $n$ -torus). *Consider the flow network problem (1.1) for  $(G, \{h_e\}_{e \in \mathcal{E}}, p_{\text{sd}}, \gamma)$  and suppose that each flow function  $h_e$ ,  $e \in \mathcal{E}$ , is monotone on the interval  $[-\gamma, \gamma]$ . Let  $\Sigma$  be a cycle basis for  $G$ ,  $\mathbf{u} \in \mathbb{Z}^{m-n+1}$ ,  $f^{(0)} \in F_{\text{sd}}$ , and  $\{f^{(k)}\}_{k \in \mathbb{Z}_{\geq 0}}$  be the sequence generated by the projection iteration (5.3) starting from  $f^{(0)}$ . Then, the following statements hold:*

- (i) *there exists a unique  $f_{\mathbf{u}}^* \in F_{\text{sd}}$  such that  $\{f^{(k)}\}_{k \in \mathbb{Z}_{\geq 0}}$  converges to  $f_{\mathbf{u}}^*$ ;*
- (ii) *for every  $k \in \mathbb{Z}_{\geq 0}$ , we have*

$$\|f^{(k+1)} - f^{(k)}\|_{L_{\min} \mathcal{A}} \leq \|I_m - L_{\min} L_{\max}^{-1}\|_\infty^k \|T_{\mathbf{u}}(f^{(0)}) - f^{(0)}\|_{L_{\min} \mathcal{A}}.$$

*Moreover, the following statements are equivalent:*

- (iii)  *$|f_{\mathbf{u}}^*|_e \leq a_{ij} |h_e(\gamma)|$ , for every  $e = (i, j) \in \mathcal{E}$ ;*
- (iv)  *$f_{\mathbf{u}}^*$  is the unique solution to the  $\mathbf{u}$ -winding balance equation (5.1);*
- (v) *for  $\theta^* = L^\dagger B \mathcal{A} (h_\gamma^{-1}(\mathcal{A}^{-1} f_{\mathbf{u}}^*) - 2\pi C_\Sigma^\dagger \mathbf{u})$ , the pair  $(f_{\mathbf{u}}^*, \theta^*)$  is the unique solution for the flow network problem (1.1) with  $\theta^* \in \Omega_{\mathbf{u}}^G$ .*

This theorem establishes that the projection iteration (5.3) correctly computes the solution of the  $\mathbf{u}$ -winding balance equation (5.1), if one exists. Moreover, the iteration does so with a convergence rate equal to  $\|I_m - L_{\min} L_{\max}^{-1}\|_\infty$  and, remarkably, this rate is independent of the network size.

We are now finally ready to present an algorithm that summarizes numerous previous results. The procedure proposed in Algorithm 5.1 is guaranteed to compute all the solutions of the flow network problem (1.1) on the  $n$ -torus, as we summarize in the next corollary.



**Algorithm 5.1 Flow Network Solver**

**Input:** a cyclic connected weighted undirected graph  $G$ , a supply/demand vector  $p_{\text{sd}}$ , an angle  $\gamma \in [0, \pi)$ , and a tolerance  $\rho > 0$  for accuracy of the flows solutions.

**Output:** all flows for (1.1)

---

```

1: compute a basis  $\{\sigma_1, \dots, \sigma_{m-n+1}\}$  for the cycle space of  $G$ 
2: for each candidate winding vector  $\mathbf{u} = (w_1, \dots, w_{m-n+1})^\top$  with  $w_i \leq \left\lfloor \frac{\gamma n_{\sigma_i}}{2\pi} \right\rfloor$  :
3:   set  $k \leftarrow 0$  and  $f^{(0)} \leftarrow \mathbb{0}_m$ 
4:   repeat
5:      $f^{(k+1)} \leftarrow T_{\mathbf{u}}(f^{(k)})$ 
6:      $k \leftarrow k + 1$ 
7:   until  $\|f^{(k)} - f^{(k-1)}\|_\infty < \rho$ 
8:   if  $|f_e^{(k)}| \leq a_{ij}|h_e(\gamma)|$ , for every  $e = (i, j) \in \mathcal{E}$  then
9:     return  $(f^{(k)}, \theta^* = L^\dagger B \mathcal{A}(h_\gamma^{-1}(\mathcal{A}^{-1} f^{(k)}) - 2\pi C_\Sigma^\dagger \mathbf{u}))$ , as the unique solution of (1.1) with  $\theta^* \in \Omega_{\mathbf{u}}^G$ .
10:  else
11:    return there exists no solution  $(f, \theta)$  for (1.1) with  $\theta \in \Omega_{\mathbf{u}}^G$ .

```

---

COROLLARY 5.3 (Complete solver for flow network problem). *Consider the flow network problem (1.1) for  $(G, \{h_e\}_{e \in \mathcal{E}}, p_{\text{sd}}, \gamma)$  and suppose that each flow function  $h_e$ ,  $e \in \mathcal{E}$ , is monotone on the interval  $[-\gamma, \gamma]$ . Then the **Flow Network Solver** in Algorithm 5.1 finds all solutions  $(f, \theta)$  for the flow network problem (1.1).*

**5.3. Computational complexity of the flow network solver.** The Flow Network Solver 5.1 consists of two main components: i) an algorithm for computing a cycle basis  $\Sigma$  (step 1:), and ii) the computation of the projection iteration for every feasible winding vector (for-loop at steps 2:-11:). Interestingly, the computational complexity of these two components are interconnected. Choosing a computationally light algorithm for computing the cycle basis (step 1:) might give rise to a cycle basis with long cycles, a large number of feasible winding vectors, and, in turn, to a large number of executions of the projection iteration (for-loop at step 2:). On the other hand, computing the cycle basis that minimizes the cardinality of feasible winding vectors can be computationally heavy. Characterizing the right trade-off is out of the scope of this paper and we leave it to the future research. In this section, we focus on the minimum cycle basis algorithms for step 1: (see Remark 3.2) and provide a detailed study of the run time of each step of the Flow Network Solver 5.1. We assume that each mathematical operation (addition, subtraction, multiplication, and division) is a single floating-point operation (flop).

THEOREM 5.4 (Computational complexity of the Flow Network Solver). *Consider the flow network problem  $(G, \{h_e\}_{e \in \mathcal{E}}, p_{\text{sd}}, \gamma)$  with monotone flow functions  $h_e$ ,  $e \in \mathcal{E}$ , on the interval  $[-\gamma, \gamma]$ . Let  $\Sigma = \{\sigma_1, \dots, \sigma_{m-n+1}\}$  be a cycle basis for  $G$ . The Flow Network Solver 5.1 has the following properties:*

- (i) *the number of times the for-loop at step 2: is invoked is  $\prod_{i=1}^{m-n+1} \left\lfloor \frac{\gamma n_{\sigma_i}}{2\pi} \right\rfloor$ ;*
- (ii) *the run time of (one execution of) steps 3:-11: (i.e., the projection iteration (5.3) with its stopping condition) is  $\mathcal{O}(\log(\rho^{-1})n^3)$ ; and*

(iii) in summary, the run time of the for-loop at steps 2:-11: is

$$\mathcal{O}\left(\log(\rho^{-1})n^3\left(\frac{\gamma}{2\pi}\right)^{m-n+1}n_{\sigma_1}\dots n_{\sigma_{m-n+1}}\right).$$

Moreover, adopting the modified Horton algorithm in [45] (see Remark 3.2) to compute the minimum cycle basis,

(iv) the run time of the Flow Network Solver 5.1 is

$$\mathcal{O}\left(m^2n/\log(n) + n^2m + \log(\rho^{-1})n^3\left(\frac{3\gamma(n-1)(n-2)}{2\pi(m-n+1)}\right)^{m-n+1}\right).$$

Several remarks are in order.

REMARK 5.5 (Bounds on the run time of Flow Network Solver).

- (i) Theorem 5.4(iv) only provides an asymptotic upper bound on the run time of Flow Network Solver 5.1. In practice, for sparse graphs with few number of cycles, this asymptotic bound is conservative.
- (ii) The run time for computing a minimal cycle basis  $\Sigma = (\sigma_1, \dots, \sigma_{m-n+1})$  in step 2: is polynomial in the number of nodes of the network (see Remark 3.2).
- (iii) For a given winding vector, the run time of the projection iteration (5.3) is cubic in the number of nodes of the network.
- (iv) For Kuramoto coupled oscillators (1.9) with identical zero natural frequencies, [69] proves that the problem of finding non-zero stable equilibrium points is NP-hard. Moreover, [69] shows that the problem remains NP-hard if it is restricted to finding non-zero equilibrium points satisfying  $|\theta_i - \theta_j| < \frac{\pi}{2}$ , for every adjacent nodes  $(i, j) \in \mathcal{E}$ . Indeed, following a similar argument as in [69], one can show that the problem of finding all solutions of the flow network problem (1.1) on the  $n$ -torus is NP-hard.
- (v) For networks with specific topologies, the run time of Flow Network Solver 5.1 can be exponential. This is illustrated in Example 5.6. The key idea is that, for appropriate network families, the number of feasible winding vectors  $(w_1, \dots, w_{m-n+1})^\top$  with  $w_i \leq \lfloor \gamma n_{\sigma_i} / 2\pi \rfloor$  grows exponentially with the number of nodes in the network.

EXAMPLE 5.6 (Exponential run time for the Flow Network Solver). Consider the flow network problem  $(G, \{h_e\}_{e \in \mathcal{E}}, 0_n, \gamma)$  with graph  $G$  as given in Figure 8, flow function  $h_e(\cdot) = \sin(\cdot)$ , for every  $e \in \mathcal{E}$ , and  $\frac{2\pi}{5} \leq \gamma \leq \frac{\pi}{2}$ .

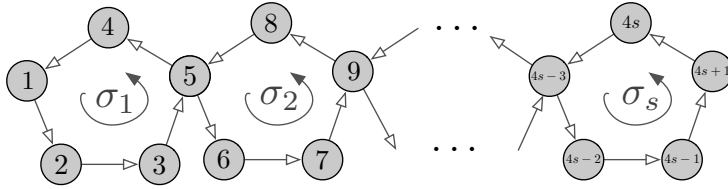


Fig. 8: The graph  $G$  with  $n = 4s + 1$  nodes,  $m = 5s$  edges, and  $s$  cycles.

We use the Flow Network Solver 5.1 to find all the solutions of the flow network problem (1.1) on the  $n$ -torus. First note that  $h_e(\cdot) = \sin(\cdot)$  is an odd monotone function on the interval  $[-\gamma, \gamma]$ . Thus, by Theorem 5.4(ii), the run time of one execution of the steps 3:-11: is  $\mathcal{O}(\log(\rho^{-1})n^3)$ . The only cycle basis for the graph  $G$

is  $\Sigma = (\sigma_1, \dots, \sigma_s)$ . Therefore, the number of times the for-loop in steps 2:-11: is invoked is  $\prod_{i=1}^s \left\lfloor \frac{\gamma^{n_{\sigma_i}}}{2\pi} \right\rfloor = 3^s = (\sqrt[4]{3})^{n-1}$ . As a result, the run time of the Flow Network Solver 5.1 is  $\mathcal{O}\left(\log(\rho^{-1})n^3(\sqrt[4]{3})^{n-1}\right)$ . Moreover, one can show that the above flow network problem has  $3^s$  solutions. Thus, the Flow Network Solver 5.1 does not find all the solutions of above flow network problem in polynomial time.

**5.4. Comparison with existing methods.** We conclude this section by comparing the Flow Network Solver 5.1 with two existing numerical algorithms for computing solutions of flow networks on the  $n$ -torus. The first algorithm is the holomorphic embedding method (HELM), which is proposed in [70] and further developed in [61] to compute all solutions of power flow equations. The second algorithm is a numerical method based on parameter homotopy, which is proposed in [46] to compute all the equilibria of the Kuramoto model.

Our approach differs from these two methods in several ways. First, these methods do not characterize the geometry of winding cells and do not explain the relationships between winding numbers, solutions, and loop flows. On the other hand, our Flow Network Solver 5.1 provides a geometric localization of the solutions based on their winding vectors. Second, while [70] and [46] do not provide a computational complexity analysis of HELM and parameter homotopy, the Flow Network Solver 5.1, based upon (i) computing a cycle basis and (ii) performing a Banach contraction, lends itself to straightforward complexity analysis. Third, both HELM and parameter homotopy method use the sinusoidal form of the flow function to reformulate the problem as a polynomial system. Therefore, these methods are not extendable to flow networks on the  $n$ -torus with arbitrary flow functions. Finally, as presented in [70] and [46], HELM and the parameter homotopy method ignore the angle constraints (1.1c) and aim to find all solutions to equations (1.1a) and (1.1b) by reformulating them as a polynomial system. Thus, for flow networks where the number of solutions of the polynomial system is much larger than the number of solutions of the flow network problem (1.1), these methods are not computationally efficient.

**6. Numerical experiments and applications.** In this section, we numerically study the solutions of the active power flow equations (1.5) with the thermal constraint (1.6) as a flow network problem on the  $n$ -torus.

**6.1. Loop flows in a simple cycle.** In this part, we consider two simple networks with the same underlying graph  $G$ , the same edge weight matrix  $\mathcal{A}$ , and different balanced power supply/demand vectors  $\widehat{p}_{sd}$  as shown in Figure (9). For each of these networks, we scale the power transmission by a scalar  $P \in \mathbb{R}_{\geq 0}$ , that is, we consider the balanced power supply/demand vectors  $p_{sd} = P\widehat{p}_{sd}$ .

Using Theorem 4.2, the active power flow equations (1.5) with thermal constraints (1.6) can only have solutions  $(f, \theta)$  with  $|w_\sigma(\theta)| \leq 3$ . For every winding number  $u \in \{0, \pm 1, \pm 2, \pm 3\}$ , we define the *power transmission capacity (PTC)* of the network at winding number  $u$  as the maximum  $P$  for which the active power flow equations (1.5) with thermal constraints (1.6) have a solutions with winding number  $u$ . Moreover, for every winding number  $u \in \{0, \pm 1, \pm 2, \pm 3\}$ , we define the maximum network congestion at winding number  $u$  by

$$\max_{e=(i,j) \in \mathcal{E}} |a_{ij}^{-1} f_e|$$

where  $(f, \theta) \in \mathbb{R}^m \times \mathbb{T}^n$  is the solution for the active power flow equations (1.5) with  $w_\sigma(\theta) = u$ .

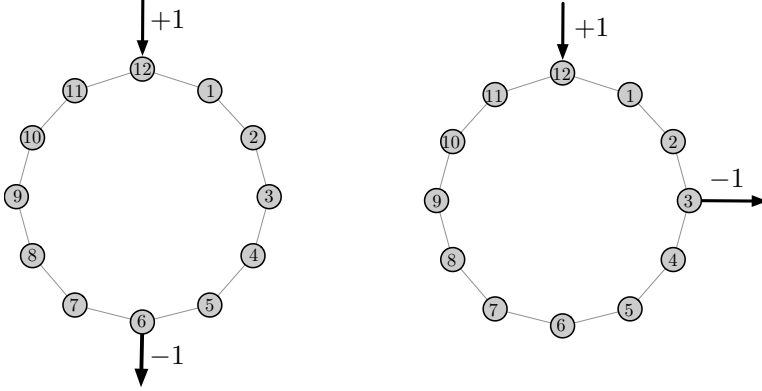


Fig. 9: Example networks. Left image: 12-node ring graph with weight matrix  $\mathcal{A} = I_{12}$  and symmetric power profile with  $\hat{p}_{sd} = [0_5^\top, -1, 0_5^\top, 1]^\top$ . Right image: 12-node ring graph with weight matrix  $\mathcal{A} = I_{12}$  and asymmetric power profile with  $\hat{p}_{sd} = [0_2^\top, -1, 0_8^\top, 1]^\top$ .

We study the effect of scaling the power transmission on the solutions of the active power flow equations (1.5) with thermal constraints (1.6). We start from  $P = 0$  and increase  $P$  by increment of  $5 \times 10^{-6}$  until the given solution of the active power flow ceases to exist. For each  $P$ , we use the Algorithm 5.1 with tolerance  $10^{-6}$  to compute the solutions of the active power flow equations (1.5) with thermal constraints (1.6). The results of this simulation are shown in Figure 10.

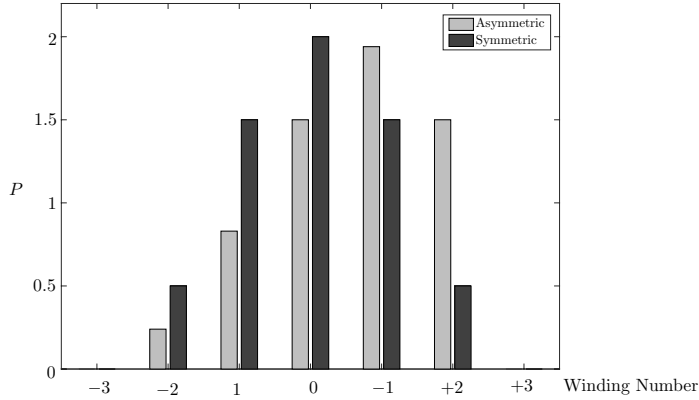


Fig. 10: Solutions of active power flow equation with different winding numbers for symmetric and asymmetric power profiles shown in Figure 9. For the symmetric power profile (left image in Figure 9) the largest power transmission capacity is for winding number 0. However, for the asymmetric power profile (middle image in Figure 9) the largest power transmission capacity is for winding number -1.

*Summary evaluation.* The winding number 0 does not necessarily carry the maximum PTC of a network. As illustrated in Figure 10, the winding number -1 carries the largest network PTC for the asymmetric supply/demand vector

$p_{sd} = P[0_2, -1, 0_8, +1]^\top$ . For the asymmetric case, more power can flow along the left path when the winding number is  $-1$  than when the winding number is  $0$ , due to the thermal constraint (1.6). As a result, when the winding number is  $-1$ , the flow along the left path of the ring is able to better relieve the capacity for the right path.  $\triangle$

**6.2. Loop flows in IEEE RTS 24 testcase.** The ongoing shift from fossil-fueled power generation to renewable energy resources is leading to large changes in the supply/demand structure of the power grids. One of the related issues is the change to undesirable operating points, where large powers are flowing over the network. In this part, we study the existence of undesirable operating points for the modified IEEE RTS 24 testcase. The IEEE RTS 24 is a portion of the larger IEEE RTS 96 testcase which is designed to study reliability of the power networks [21]. This testcase can be described by a connected, undirected graph  $G$  with 24 buses and 34 branches. The nodal admittance matrix is denoted by  $Y \in \mathbb{C}^{24 \times 24}$ . The set of nodes are partitioned into load buses  $\mathcal{V}_1$  and generator buses  $\mathcal{V}_2$ . The power demand (resp. power supply) at node  $i \in \mathcal{V}_1$  (resp.  $\mathcal{V}_2$ ) is denoted by the  $i$ th element of  $p_{sd}$ . The nominal parameters for the test cases can be found in [21] and is shown in the second column of the Table (2). We first modify the branches in IEEE RTS 24 to be lossless without shunt admittances. Since our theoretical results assume that all nodes are  $PV$  nodes, MATPOWER's solver is used to compute the voltage magnitudes at every node [75]. Then the edge weights of  $G$  are set to  $a_{ij} = a_{ji} = V_i V_j \text{Im}(Y_{ij}) > 0$ . A cycle basis for  $G$  is  $\Sigma = \{\sigma_1, \dots, \sigma_{11}\}$  where, for every  $i \in \{1, \dots, 11\}$ , the cycle  $\sigma_i$  is given in Table 1.

Cycle basis for IEEE RTS 24	
$\sigma_1 = (2, 1, 3, 9, 4, 2)$	$\sigma_2 = (5, 1, 3, 9, 8, 10, 5)$
$\sigma_3 = (10, 6, 2, 4, 9, 8, 10)$	$\sigma_4 = (11, 10, 8, 9, 11)$
$\sigma_5 = (12, 10, 8, 9, 12)$	$\sigma_6 = (13, 11, 9, 12, 23, 13)$
$\sigma_7 = (13, 12, 23, 13)$	$\sigma_8 = (16, 15, 24, 3, 9, 11, 14, 16)$
$\sigma_9 = (21, 15, 24, 3, 9, 11, 14, 16, 17, 22, 21)$	$\sigma_{10} = (21, 18, 17, 22, 21)$
$\sigma_{11} = (23, 20, 19, 16, 14, 11, 9, 12, 23)$	

Table 1: A cycle basis  $\Sigma$  for the IEEE RTS 24 testcase

We also modify the nominal power supply/demand of the IEEE RTS 24 testcase. The goal is to increase the penetration of renewable energy units and remove some of the synchronous generators. Our modification in the power supply/demand of the IEEE RTS 24 testcase is illustrated in Figure 11. The modified supply/demand vector is denoted by  $p_{sd}^{\text{mod}}$  and is given in the third column of Table 2.

Using the Algorithm 5.1, we study the active power flow equation (1.5) and the thermal constraints (1.6) with maximum power angle  $\gamma = 1.5$  rad. First, we observe that, for the nominal power supply/demand vector of IEEE RTS 24, there exists no solution for this problem with a nonzero winding vector. However, for the modified supply/demand vector  $p_{sd}^{\text{mod}}$ , there exists exactly one solution associated to the winding vector  $\mathbf{u} = \mathbf{0}_{11}$  and one solution associated to the winding vector  $\mathbf{u} = [\mathbf{0}_{10}^\top, -1]^\top$ . We then examine the computational efficiency of the projection iteration (5.3) for checking the existence/finding solutions of the active power flow equations (1.5). We assume that the cycle basis  $\Sigma$  illustrated in Table 1 is given. For every winding vector  $\mathbf{u} \in \text{Im}(\mathbf{w}_\Sigma)$ , we focus on the  $\mathbf{u}$ -winding balance equations (5.1). Then  $t_{\text{fsolve}}$  is the computational time for solving (5.1) using MATLAB's fsolve and  $t_{\text{sequence}}$  is the com-

putational time for solving (5.1) using the projection iteration (5.3). For  $\mathbf{u} = \mathbf{0}_{11}$  and  $\mathbf{u} = [\mathbf{0}_{10}^\top, -1]$ , the computational times  $t_{\text{sequence}}$  and  $t_{\text{fsolve}}$  are compared in Table (3).<sup>1</sup>

IEEE RTS 24					
Node	$p_{\text{sd}}^{\text{nom}}$ (MW)	$p_{\text{sd}}^{\text{mod}}$ (MW)	Node	$p_{\text{sd}}^{\text{nom}}$ (MW)	$p_{\text{sd}}^{\text{mod}}$ (MW)
1	64.00	8.40	13	-129.00	-193.50
2	75.00	9.27	14	-194.00	-143.39
3	-180.00	-268.48	15	-102.00	-153.00
4	-74.00	-99.14	16	55.00	00.00
5	-71.00	-79.96	17	00.00	00.00
6	-136.00	-68.63	18	67.00	00.00
7	115.00	63.65	19	-181.00	26.57
8	-171.00	-142.41	20	-128.00	100.00
9	-175.00	-245.21	21	400.00	00.00
10	-195.00	95.83	22	300.00	00.00
11	00.00	100.00	23	660.00	990.00
12	00.00	00.00	24	00.00	00.00

Table 2: Nominal supply/demand vector  $p_{\text{sd}}^{\text{nom}}$  versus modified supply/demand vector  $p_{\text{sd}}^{\text{mod}}$ .

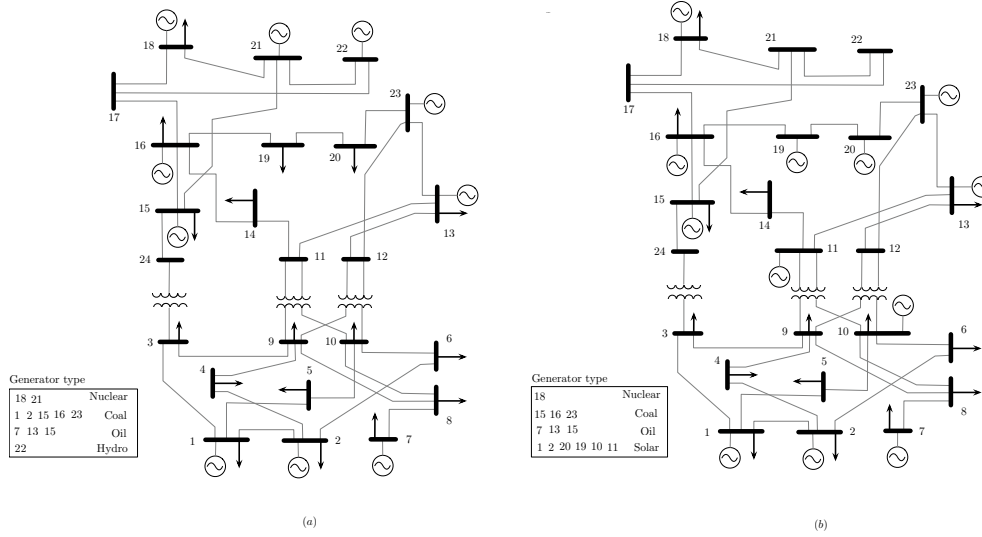


Fig. 11: (a) shows the original IEEE RTS 24 test case with generator types and (b) shows the modified IEEE RTS 24 test case. The modifications in power supply/demand vector in Figure (b) are: i) shutting down the hydro generator at node 22, the thermal generators at node 1 and 2, and the nuclear generator at node 21 ii) adding solar energy generations at nodes 1,2, 10, 11, 19, 20, 23.

<sup>1</sup>The computer specifications for these simulations are as follows: Processor Intel Core i5 @ 1.6 GHZ CPU and 4 GB RAM.



Winding vector, $\mathbf{u}$	$t_{\text{sequence}}/t_{\text{fsolve}}$
$[0_{11}^T]$	0.2463
$[0_{10}^T, -1]$	0.0788

Table 3: Computation time for the projection iteration (5.3) for  $\gamma = 1.5$  is denoted by  $t_{\text{sequence}}$  and for MATLAB’s *fsolve* is denoted by  $t_{\text{fsolve}}$ . The values given in the table are the ratio  $t_{\text{sequence}}/t_{\text{fsolve}}$ , averaged over 5 trials. The computations use a tolerance of  $10^{-6}$ .

*Summary evaluation.* We used the Algorithm 5.1 to check for the existence/find all solutions of the active power flow equations (1.5) for the nominal and modified IEEE RTS 24 testcase. Table 3 shows that, for the nominal and modified IEEE RTS 24 testcase, the projection iteration (5.3) not only converges to the loop flow solutions but also is faster than the MATLAB’s *fsolve* for checking the existence/computing the solutions of the active power flow equations.  $\triangle$

**7. Conclusion.** In this paper, we have introduced two classes of network problems on the  $n$ -torus—flow networks and elastic networks—and we developed a rigorous framework to study the multiple solutions of these problems. We extended Kirchoff’s voltage law to networks with phase-valued (instead of real-valued) nodal variables, and we showed how this law induces a partition of the  $n$ -torus into winding cells. We demonstrated that these winding cells localize solutions of the flow and elastic network problems, since each cell contains at most one solution. In order to compute the solution in each winding cell (or determine that no solution exists), we proposed the projection iteration, a novel contraction mapping. Finally, we presented several numerical experiments, which investigate the notion of flow capacity and flow congestion in different test cases, and we verified the accuracy and efficiency of our methods.

Much work remains on the connection of solutions of flow and elastic networks with other phenomena in network systems. For power systems specifically, we have already exploited the winding partition to derive sufficient conditions for transient stability in AC grids [66]. But this work assumes lossless AC grids with constant voltage magnitudes, and it is important to investigate power flows in more realistic scenarios. See [64, 6] for recent work in this direction. It would also be interesting to compare the performance of our Flow Network Solver 5.1 to state-of-the-art power flow solvers in the literature. Other numerical directions include applying our flow network solver to study collective motion in engineering networks and the performance of associative memory networks. In a more theoretical direction, it would be valuable to apply the framework and analysis of this paper to study more general coupled oscillator networks, such as FitzHugh–Nagumo and Hodgkin–Huxley models [13, 43, 18]. In particular, we envision that the winding partition may be useful in developing analytic conditions for synchronization in coupled oscillator networks, which is one of the central problems in this area of research [49, 8, 14].

## REFERENCES

- [1] R. Abraham, J. E. Marsden, and T. S. Ratiu. *Manifolds, Tensor Analysis, and Applications*, volume 75 of *Applied Mathematical Sciences*. Springer, 2 edition, 1988.
- [2] J. W. Alexander. Topological invariants of knots and links. *Transactions of the American Mathematical Society*, 30(2):275–306, 1928. doi:10.2307/1989123.
- [3] J. Baillieul and C. I. Byrnes. Geometric critical point analysis of lossless power system models. *IEEE Transactions on Circuits and Systems*, 29(11):724–737, 1982. doi:10.1109/TCS.

- 1982.1085093.
- [4] A. R. Bergen and D. J. Hill. A structure preserving model for power system stability analysis. *IEEE Transactions on Power Apparatus and Systems*, 100(1):25–35, 1981. doi:10.1109/TPAS.1981.316883.
  - [5] N. Biggs. Algebraic potential theory on graphs. *Bulletin of the London Mathematical Society*, 29(6):641–682, 1997. doi:10.1112/S0024609397003305.
  - [6] J. C. Bronski, T. Carty, and L. DeVille. Configurational stability for the Kuramoto–Sakaguchi model. *Chaos: An Interdisciplinary Journal of Nonlinear Science*, 28(10):103109, 2018. doi:10.1063/1.5029397.
  - [7] F. Bullo. *Lectures on Network Systems*. Kindle Direct Publishing, 1.4 edition, July 2020. With contributions by J. Cortés, F. Dörfler, and S. Martínez. URL: <http://motion.me.ucsb.edu/book-lns>.
  - [8] N. Chopra and M. W. Spong. On exponential synchronization of Kuramoto oscillators. *IEEE Transactions on Automatic Control*, 54(2):353–357, 2009. doi:10.1109/TAC.2008.2007884.
  - [9] T. Coletta, R. Delabays, I. Adagideli, and P. Jacquod. Topologically protected loop flows in high voltage AC power grids. *New Journal of Physics*, 18(10):103042, 2016. doi:10.1088/1367-2630/18/10/103042.
  - [10] O. Coss, J. D. Hauenstein, H. Hong, and D. K. Molzahn. Locating and counting equilibria of the Kuramoto model with rank-one coupling. *SIAM Journal on Applied Algebra and Geometry*, 2(1):45–71, 2018. doi:10.1137/17M1128198.
  - [11] H. Daido. Quasientrainment and slow relaxation in a population of oscillators with random and frustrated interactions. *Physical Review Letters*, 68(7):1073–1076, 1992. doi:10.1103/PhysRevLett.68.1073.
  - [12] R. Delabays, T. Coletta, and P. Jacquod. Multistability of phase-locking and topological winding numbers in locally coupled Kuramoto models on single-loop networks. *Journal of Mathematical Physics*, 57(3):032701, 2016. doi:10.1063/1.4943296.
  - [13] M. Desroches, J. Guckenheimer, B. Krauskopf, C. Kuehn, H. Osinga, and M. Wechselberger. Mixed-mode oscillations with multiple time scales. *SIAM Review*, 54(2):211–288, 2012. doi:10.1137/100791233.
  - [14] F. Dörfler, M. Chertkov, and F. Bullo. Synchronization in complex oscillator networks and smart grids. *Proceedings of the National Academy of Sciences*, 110(6):2005–2010, 2013. doi:10.1073/pnas.1212134110.
  - [15] M. Elkin, C. Liebchen, and R. Rizzi. New length bounds for cycle bases. *Information Processing Letters*, 104(5):186–193, 2007. doi:10.1016/j.ipl.2007.06.013.
  - [16] G. B. Ermentrout. The behavior of rings of coupled oscillators. *Journal of Mathematical Biology*, 23(1):55–74, 1985. doi:10.1007/BF00276558.
  - [17] T. Fergusson. Topological states in the Kuramoto model. *SIAM Journal on Applied Dynamical Systems*, 17(1):484–499, 2018. doi:10.1137/17M112484X.
  - [18] A. Franci, G. Drion, and R. Sepulchre. Modeling the modulation of neuronal bursting: A singularity theory approach. *SIAM Journal on Applied Dynamical Systems*, 13(2):798–829, 2014. doi:10.1137/13092263X.
  - [19] C. D. Godsil and G. F. Royle. *Algebraic Graph Theory*. Springer, 2001.
  - [20] G. H. Golub and C. F. van Loan. *Matrix Computations*. Johns Hopkins University Press, 2 edition, 1989.
  - [21] C. Grigg et al. The IEEE Reliability Test System-1996. A report prepared by the Reliability Test System Task Force of the Application of Probability Methods Subcommittee. *IEEE Transactions on Power Systems*, 14(3):1010–1020, 1999. doi:10.1109/59.780914.
  - [22] NERC Steering Group. Technical Analysis of the August 14, 2003, Blackout: What Happened, Why, and What Did We Learn? Technical report, North American Electric Reliability Council, Princeton Forrestal Village, Princeton, NJ, USA, July 2004.
  - [23] V. Guillemin and A. Pollack. *Differential Topology*. American Mathematical Society, 2010.
  - [24] J. J. Hopfield. Neural networks and physical systems with emergent collective computational abilities. *Proceedings of the National Academy of Sciences*, 79(8):2554–2558, 1982. doi:10.1073/pnas.79.8.2554.
  - [25] F. C. Hoppensteadt and E. M. Izhikevich. Synchronization of laser oscillators, associative memory, and optical neurocomputing. *Physical Review E*, 62(3):4010–4013, 2000. doi:10.1103/PhysRevE.62.4010.
  - [26] R. A. Horn and C. R. Johnson. *Matrix Analysis*. Cambridge University Press, 2nd edition, 2012.
  - [27] J. D. Horton. A polynomial-time algorithm to find the shortest cycle basis of a graph. *SIAM Journal on Computing*, 16(2):358–366, 1987. doi:10.1137/0216026.

- [28] S. Jafarpour and F. Bullo. Synchronization of Kuramoto oscillators via cutset projections. *IEEE Transactions on Automatic Control*, 64(7):2830–2844, 2019. doi:10.1109/TAC.2018.2876786.
- [29] N. Janssens and A. Kamagate. Loop flows in a ring AC power system. *International Journal of Electrical Power & Energy Systems*, 25(8):591–597, 2003. doi:10.1016/S0142-0615(03)00017-6.
- [30] T. Kavitha, C. Liebchen, K. Mehlhorn, D. Michail, R. Rizzi, T. Ueckerdt, and K. A. Zweig. Cycle bases in graphs characterization, algorithms, complexity, and applications. *Computer Science Review*, 3(4):199–243, 2009. doi:10.1016/j.cosrev.2009.08.001.
- [31] A. J. Korsak. On the question of uniqueness of stable load-flow solutions. *IEEE Transactions on Power Apparatus and Systems*, 91(3):1093–1100, 1972. doi:10.1109/TPAS.1972.293463.
- [32] A. Kumar, R. Mudumbai, S. Dasgupta, M. M. Rahman, D. R. Brown III, U. Madhow, and T. P. Bidigare. A scalable feedback mechanism for distributed nullforming with phase-only adaptation. *IEEE Transactions on Signal and Information Processing over Networks*, 1(1):58–70, 2015. doi:10.1109/TSIPN.2015.2442921.
- [33] Y. Kuramoto. *Chemical Oscillations, Waves, and Turbulence*. Springer, 1984.
- [34] F. Lazebnik. On systems of linear Diophantine equations. *Mathematics Magazine*, 69(4):261–266, 1996. doi:10.2307/2690528.
- [35] N. E. Leonard, D. Paley, F. Lekien, R. Sepulchre, D. M. Fratantoni, and R. Davis. Collective motion, sensor networks and ocean sampling. *Proceedings of the IEEE*, 95(1):48–74, 2007.
- [36] B. Lesieutre and D. Wu. An efficient method to locate all the load flow solutions - revisited. In *Allerton Conf. on Communications, Control and Computing*, pages 381–388, Monticello, IL, USA, October 2015. doi:10.1109/ALLERTON.2015.7447029.
- [37] S. Ling, R. Xu, and A. S. Bandeira. On the landscape of synchronization networks: A perspective from nonconvex optimization. *SIAM Journal on Optimization*, 29(3):1879–1907, 2019. doi:10.1137/18M1217644.
- [38] S. H. Low. Convex relaxation of optimal power flow — Part I: Formulations and equivalence. *IEEE Transactions on Control of Network Systems*, 1(1):15–27, 2014. doi:10.1109/TCNS.2014.2309732.
- [39] W. Ma and J. S. Thorp. An efficient algorithm to locate all the load flow solutions. *IEEE Transactions on Power Systems*, 8(3):1077–1083, 1993. doi:10.1109/59.260891.
- [40] D. Manik, M. Timme, and D. Witthaut. Cycle flows and multistability in oscillatory networks. *Chaos: An Interdisciplinary Journal of Nonlinear Science*, 27(8):083123, 2017. doi:10.1063/1.4994177.
- [41] M. H. Matheny et al. Exotic states in a simple network of nanoelectromechanical oscillators. *Science*, 363(6431), 2019. doi:10.1126/science.aav7932.
- [42] G. S. Medvedev. Small-world networks of Kuramoto oscillators. *Physica D: Nonlinear Phenomena*, 266:13–22, 2014. doi:10.1016/j.physd.2013.09.008.
- [43] G. S. Medvedev and N. Kopell. Synchronization and transient dynamics in the chains of electrically coupled Fitzhugh-Nagumo oscillators. *SIAM Journal on Applied Mathematics*, 61(5):1762–1801, 2001. doi:10.1137/S0036139900368807.
- [44] G. S. Medvedev and X. Tang. Stability of twisted states in the Kuramoto model on Cayley and random graphs. *Journal of Nonlinear Science*, 25(6):1169–1208, 2015. doi:10.1007/s00332-015-9252-y.
- [45] K. Mehlhorn and D. Michail. Minimum cycle bases: Faster and simpler. *ACM Transactions on Algorithms*, 6(1):8:1–8:13, 2009. doi:10.1145/1644015.1644023.
- [46] D. Mehta, N. S. Daleo, F. Dörfler, and J. D. Hauenstein. Algebraic geometrization of the Kuramoto model: Equilibria and stability analysis. *Chaos: An Interdisciplinary Journal of Nonlinear Science*, 25(5):053103, 2015. doi:10.1063/1.4919696.
- [47] D. C. Michaels, E. P. Matyas, and J. Jalife. Mechanisms of sinoatrial pacemaker synchronization: A new hypothesis. *Circulation Research*, 61(5):704–714, 1987. doi:10.1161/01.RES.61.5.704.
- [48] J. W. Milnor. *Topology from the Differentiable Viewpoint*. Princeton University Press, 1997. Reprint of 1965 edition.
- [49] R. E. Mirollo and S. H. Strogatz. The spectrum of the locked state for the Kuramoto model of coupled oscillators. *Physica D: Nonlinear Phenomena*, 205(1-4):249–266, 2005. doi:10.1016/j.physd.2005.01.017.
- [50] A. Mirzaei, M. E. Heidari, R. Bagheri, S. Chehraz, and A. A. Abidi. The quadrature LC oscillator: A complete portrait based on injection locking. *IEEE Journal of Solid-State Circuits*, 42(9):1916–1932, 2007. doi:10.1109/JSSC.2007.903047.
- [51] D. K. Molzahn, F. Dörfler, H. Sandberg, S. H. Low, S. Chakrabarti, R. Baldick, and J. Lavaei. A survey of distributed optimization and control algorithms for electric power systems. *IEEE*

- Transactions on Smart Grid*, 8(6):2941–2962, 2017. doi:10.1109/TSG.2017.2720471.
- [52] D. K. Molzahn, B. C. Lesieutre, and H. Chen. Counterexample to a continuation-based algorithm for finding all power flow solutions. *IEEE Transactions on Power Systems*, 28(1):564–565, 2013. doi:10.1109/TPWRS.2012.2202205.
  - [53] J. A. Momoh, R. Adapa, and M. E. El-Hawary. A review of selected optimal power flow literature to 1993. I. Nonlinear and quadratic programming approaches. *IEEE Transactions on Power Systems*, 14(1):96–104, 1999. doi:10.1109/59.744492.
  - [54] J. A. Momoh, M. E. El-Hawary, and R. Adapa. A review of selected optimal power flow literature to 1993. II. Newton, linear programming and interior point methods. *IEEE Transactions on Power Systems*, 14(1):105–111, 1999. doi:10.1109/59.744495.
  - [55] J. Munkres. *Topology*. Pearson, 2 edition, 2000.
  - [56] J. C. Neu. Coupled chemical oscillators. *SIAM Journal on Applied Mathematics*, 37(2):307–315, 1979. doi:10.1137/0137022.
  - [57] T. Nishikawa, Y.-C. Lai, and F. C. Hoppensteadt. Capacity of oscillatory associative-memory networks with error-free retrieval. *Physical Review Letters*, 92:108101, 2004. doi:10.1103/PhysRevLett.92.108101.
  - [58] J. Ochab and P. F. Góra. Synchronization of coupled oscillators in a local one-dimensional Kuramoto model. *Acta Physica Polonica. Series B, Proceedings Series*, 3(2):453–462, 2010. URL: <https://www.actaphys.uj.edu.pl/S/3/2/453>.
  - [59] D. A. Paley, N. E. Leonard, R. Sepulchre, D. Grunbaum, and J. K. Parrish. Oscillator models and collective motion. *IEEE Control Systems*, 27(4):89–105, 2007. doi:10.1109/MCS.2007.384123.
  - [60] A. Pluchino, V. Latora, and A. Rapisarda. Changing opinions in a changing world: a new perspective in sociophysics. *International Journal of Modern Physics C*, 16(04):515–531, 2005. doi:10.1142/S0129183105007261.
  - [61] S. Rao, Y. Feng, D. J. Tylavsky, and J. K. Subramanian. The holomorphic embedding method applied to the power-flow problem. *IEEE Transactions on Power Systems*, 31(5):3816–3828, 2016. doi:10.1109/TPWRS.2015.2503423.
  - [62] J. A. Rogge and D. Aeyels. Stability of phase locking in a ring of unidirectionally coupled oscillators. *Journal of Physics A: Mathematical and General*, 37(46):11135–11148, 2004. doi:10.1088/0305-4470/37/46/004.
  - [63] R. Sepulchre, D. A. Paley, and N. E. Leonard. Stabilization of planar collective motion: All-to-all communication. *IEEE Transactions on Automatic Control*, 52(5):811–824, 2007. doi:10.1109/TAC.2007.898077.
  - [64] J. W. Simpson-Porco. A theory of solvability for lossless power flow equations – Part I: Fixed-point power flow. *IEEE Transactions on Control of Network Systems*, 5(3):1361–1372, 2018. doi:10.1109/TCNS.2017.2711433.
  - [65] J. W. Simpson-Porco, F. Dörfler, and F. Bullo. Synchronization and power sharing for droop-controlled inverters in islanded microgrids. *Automatica*, 49(9):2603–2611, 2013. doi:10.1016/j.automatica.2013.05.018.
  - [66] K. D. Smith, S. Jafarpour, and F. Bullo. Transient stability of droop-controlled inverter networks with operating constraints. *IEEE Transactions on Automatic Control*, July 2019. Submitted. URL: <http://arxiv.org/pdf/1907.05532>.
  - [67] P. A. Tass. A model of desynchronizing deep brain stimulation with a demand-controlled coordinated reset of neural subpopulations. *Biological Cybernetics*, 89(2):81–88, 2003. doi:10.1007/s00422-003-0425-7.
  - [68] R. Taylor. There is no non-zero stable fixed point for dense networks in the homogeneous Kuramoto model. *Journal of Physics A: Mathematical and Theoretical*, 45(5):1–15, 2012. doi:10.1088/1751-8113/45/5/055102.
  - [69] R. Taylor. Finding non-zero stable fixed points of the weighted Kuramoto model is NP-hard, 2015. ArXiv e-print. URL: <https://arxiv.org/pdf/1502.06688>.
  - [70] A. Trias. The holomorphic embedding load flow method. In *IEEE Power & Energy Society General Meeting*, pages 1–8, 2012. doi:10.1109/PESGM.2012.6344759.
  - [71] F. Varela, J. P. Lachaux, E. Rodriguez, and J. Martinerie. The brainweb: Phase synchronization and large-scale integration. *Nature Reviews Neuroscience*, 2(4):229–239, 2001. doi:10.1038/35067550.
  - [72] T. Vicsek, A. Czirók, E. Ben-Jacob, I. Cohen, and O. Shochet. Novel type of phase transition in a system of self-driven particles. *Physical Review Letters*, 75(6-7):1226–1229, 1995. doi:10.1103/PhysRevLett.75.1226.
  - [73] K. Wiesenfeld, P. Colet, and S. H. Strogatz. Frequency locking in Josephson arrays: Connection with the Kuramoto model. *Physical Review E*, 57(2):1563–1569, 1998. doi:10.1103/PhysRevE.57.1563.

- [74] D. A. Wiley, S. H. Strogatz, and M. Girvan. The size of the sync basin. *Chaos: An Interdisciplinary Journal of Nonlinear Science*, 16(1):015103, 2006. doi:10.1063/1.2165594.
- [75] R. D. Zimmerman, C. E. Murillo-Sánchez, and R. J. Thomas. MATPOWER: Steady-state operations, planning, and analysis tools for power systems research and education. *IEEE Transactions on Power Systems*, 26(1):12–19, 2011. doi:10.1109/TPWRS.2010.2051168.

### Appendix A. Two useful lemmas.

LEMMA A.1 (Properties of the cycle-edge matrix). *Given a cyclic connected undirected graph  $G$  with cycle basis  $\Sigma = \{\sigma_1, \dots, \sigma_{m-n+1}\}$ , the following statements hold:*

- (i) *the matrix  $C_\Sigma$  is of rank  $m - n + 1$ ,*
- (ii)  *$\text{Ker}(C_\Sigma) = \text{Img}(B^\top)$ ,*
- (iii) *the system of equations  $C_\Sigma \mathbf{z} = \mathbf{v}$ , for  $\mathbf{v} \in \text{Img}(\mathbf{w}_\Sigma)$ , has an integer solution.*

*Proof.* Regarding part (i), note that rank of the matrix  $C_\Sigma$  is equal to the number of linearly independent rows in  $C_\Sigma$ . By definition, the set  $\{\sigma_1, \dots, \sigma_{m-n+1}\}$  consists of linearly independent vectors in  $\mathbb{R}^m$  and thus rank of  $C_\Sigma$  is equal to  $m - n + 1$ .

Regarding part (ii), we first show that  $\text{Img}(B^\top) \subseteq \text{Ker}(C_\Sigma)$ . Suppose that  $\mathbf{y} \in \text{Img}(B^\top)$ . Then there exists  $\mathbf{x} \in \mathbb{R}^n$  such that  $\mathbf{y} = B^\top \mathbf{x}$ . Thus, for every  $i \in \{1, \dots, m - n + 1\}$ , we get

$$v_{\sigma_i}^\top \mathbf{y} = v_{\sigma_i}^\top B^\top \mathbf{x} = (B v_{\sigma_i})^\top \mathbf{x} = 0,$$

where the last equality holds since  $v_\sigma \in \text{Ker}(B)$ , for every cycle  $\sigma$ . This means that  $C_\Sigma \mathbf{y} = 0$  or equivalently  $\mathbf{y} \in \text{Ker}(C_\Sigma)$ . Therefore,  $\text{Img}(B^\top) \subseteq \text{Ker}(C_\Sigma)$ . In turn, using the result in part (i), rank of the matrix  $C_\Sigma$  is  $m - n + 1$ . Thus, by the rank-nullity theorem, we have

$$\dim(\text{Ker}(C_\Sigma)) = m - (m - n + 1) = n - 1 = \dim(\text{Img}(B^\top)).$$

As a result, we have  $\text{Img}(B^\top) = \text{Ker}(C_\Sigma)$ .

Regarding part (iii), suppose that  $\Sigma'$  is an integral cycle basis for  $G$  (for a definition and existence of an integral cycle basis see [30]). Since  $\Sigma$  is a cycle basis for  $G$ , there exists an invertible integer matrix  $T \in \mathbb{R}^{(m-n+1) \times (m-n+1)}$  such that

$$v_{\sigma'_i} = \sum_{j=1}^n t_{ji} v_{\sigma_j}.$$

This implies that  $C_{\Sigma'} = T C_\Sigma$ . We first show that the system of linear equations  $C_{\Sigma'} \mathbf{z} = T \mathbf{u}$  has an integer solution. Note that rank of the matrix  $C_{\Sigma'}$  is  $m - n + 1$ . Let  $\mathcal{T}$  be a spanning tree in  $G$  and without loss of generality, assume that the first  $m - n + 1$  column of  $C_{\Sigma'}$  are associated with the edges that are not in the spanning tree  $\mathcal{T}$ . Then, we define the matrix  $\widehat{C}_{\Sigma'} \in \mathbb{R}^{(m-n+1) \times (m-n+1)}$  as follows:

$$\widehat{C}_{\Sigma'} = [(C_{\Sigma'})_1 \quad \dots \quad (C_{\Sigma'})_{m-n+1}].$$

where  $(C_{\Sigma'})_i$  the  $i$ th column of the matrix  $C_{\Sigma'}$ . Since  $\Sigma'$  is an integral base, by [30, Theorem 3.4], we have  $|\det(\widehat{C}_{\Sigma'})| = 1$ . Since the matrix  $\widehat{C}_{\Sigma'}$  has integer entries, by [34, Theorem 1], there exists matrices  $U, V \in \mathbb{Z}^{(m-n+1) \times (m-n+1)}$  with  $|\det(U)| = |\det(V)| = 1$  such that

$$U \widehat{C}_{\Sigma'} V = B = \text{diag}(b_1, \dots, b_{m-n+1}),$$

where  $b_i$  are positive integers and  $b_i | b_{i+1}$ , for every  $i \in \{1, \dots, m-n\}$ . Note that  $|\det(\widehat{C}_{\Sigma'})| = 1$  implies that  $|\det(B)| = 1$  which in turn implies that  $|b_i| = 1$ , for every  $i \in \{1, \dots, m-n+1\}$ . Therefore, by [34, Proposition 2], for every  $\mathbf{v} \in \mathbb{Z}^{(m-n+1)}$ , there exists an integer solution  $\mathbf{x} \in \mathbb{Z}^{(m-n+1)}$  such that  $\widehat{C}_{\Sigma'}(\mathbf{x}) = T\mathbf{u}$ . Then it is straightforward to see that the integer vector  $\mathbf{z} \in \mathbb{Z}^m$  defined by  $\mathbf{z} = \begin{bmatrix} \mathbf{x} \\ \mathbf{0}_{n-1} \end{bmatrix}$  is a solution for the system of equations  $C_{\Sigma'}\mathbf{z} = T\mathbf{u}$ . This means that  $TC_{\Sigma'}\mathbf{z} = T\mathbf{u}$  and since  $T$  is invertible, we have  $C_{\Sigma'}\mathbf{z} = \mathbf{u}$ . This completes the proof of Lemma A.1.  $\square$

**LEMMA A.2** (Properties of  $D$ -weighted cycle projection). *Let  $G$  be an undirected weighted connected graph with incidence matrix  $B$  and diagonal weight matrix  $\mathcal{A} \in \mathbb{R}^{m \times m}$ . Let  $D \in \mathbb{R}^{m \times m}$  be a positive definite diagonal matrix, and  $\mathcal{P}_D$  be the  $D$ -weighted cycle projection defined in (2.2). Then the following statements hold:*

- (i)  $\mathcal{P}_D$  is idempotent;
- (ii) the eigenvalues of  $\mathcal{P}_D$  are 0 and 1 with algebraic (geometric) multiplicity  $n-1$  and  $m-n+1$ , respectively;
- (iii)  $\text{Ker}(\mathcal{P}_D D \mathcal{A}) = \text{Img}(B^\top)$ .

*Proof.* Regarding part (i), define the graph  $G'$  with the same node set, the same edge set as  $G$ , and with the diagonal weight matrix  $D\mathcal{A}$ . Clearly,  $G$  is connected if and only if  $G'$  is connected. Moreover, by [28, Theorem 4],  $\mathcal{P}_D$  is an oblique projection onto  $\text{Ker}(B D \mathcal{A})$  parallel to  $\text{Img}(B^\top)$  and, therefore, is idempotent. Regarding part (ii), the result follows from [28, Theorem 4]. Regarding part (iii), suppose that  $\alpha \in \text{Img}(B^\top)$ . This means that there exists  $\xi \in \mathbb{R}^n$  such that  $B^\top \xi = \alpha$ . As a result,

$$\begin{aligned} \mathcal{P}_D D \mathcal{A} \alpha &= D \mathcal{A} \alpha - D A B^\top (B D A B^\top)^\dagger B D \mathcal{A} \alpha = D \mathcal{A} \alpha - D A B^\top (B D A B^\top)^\dagger B D A B^\top \xi \\ &= D \mathcal{A} \alpha - D A B^\top (I_n - \frac{1}{n} \mathbf{1}_n \mathbf{1}_n^\top) \xi, \end{aligned}$$

where, for the last equality, we used the equality  $(B D A B^\top)^\dagger B D A B^\top = I_n - \frac{1}{n} \mathbf{1}_n \mathbf{1}_n^\top$ . This equality holds by the identity in [7, Lemma 6.12(iii)] and the fact that the graph  $G'$  is connected with the Laplacian matrix  $B D A B^\top$  [7, Lemma 9.1]. Note that  $B^\top \mathbf{1}_n = \mathbf{0}_m$  [7, Section 9.1]. Thus, we get

$$\mathcal{P}_D D \mathcal{A} \alpha = D \mathcal{A} \alpha - D A B^\top (I_n - \frac{1}{n} \mathbf{1}_n \mathbf{1}_n^\top) \xi = D \mathcal{A} \alpha - D A B^\top \xi = D \mathcal{A} \alpha - D \mathcal{A} \alpha = \mathbf{0}_m.$$

Therefore,  $\alpha \in \text{Ker}(\mathcal{P}_D D \mathcal{A})$  and, in turn,  $\text{Img}(B^\top) \subseteq \text{Ker}(\mathcal{P}_D D \mathcal{A})$ . Now suppose that  $\alpha \in \text{Ker}(\mathcal{P}_D D \mathcal{A})$ . Therefore,

$$\mathbf{0}_m = \mathcal{P}_D D \mathcal{A} \alpha = D \mathcal{A} \alpha - D A B^\top (B D A B^\top)^\dagger B D \mathcal{A} \alpha.$$

Note that  $\mathcal{A}$  and  $D$  are invertible. Thus,  $\alpha = B^\top (B D A B^\top)^\dagger B D \mathcal{A} \alpha$ . This implies that  $\alpha \in \text{Img}(B^\top)$  and therefore  $\text{Ker}(\mathcal{P}_D D \mathcal{A}) \subseteq \text{Img}(B^\top)$ . This completes the proof of part (iii).  $\square$

## Appendix B. Basis-independent winding map.

One can define a basis-independent winding map on  $\mathbb{T}_0^n$ . Let  $\text{Ker}'(B)$  be the dual space of the cycle space  $\text{Ker}(B)$  and let  $\Sigma' = \{v'_{\sigma_1}, \dots, v'_{\sigma_{m-n+1}}\}$  be the dual basis on  $\text{Ker}'(B)$ , associated to the basis  $\Sigma = \{v_{\sigma_1}, \dots, v_{\sigma_{m-n+1}}\}$  on  $\text{Ker}(B)$ , that is, for every  $i, j \in \{1, \dots, m-n+1\}$ , we have  $v'_{\sigma_i}(v_{\sigma_j}) = \delta_{ij}$ . Define the winding map  $\mathbf{w} : \mathbb{T}_0^n \rightarrow \text{Ker}'(B)$  by:

$$(B.1) \quad \mathbf{w}(\theta) = \frac{1}{2\pi} \sum_{i=1}^{m-n+1} (v_{\sigma_i}^\top (B^\top \theta)) v'_{\sigma_i},$$



where the vector  $(B^\top \theta)$  is defined in equation (2.3). The winding map  $\mathbf{w}_\Sigma$  in Definition 3.1(ii) is the representation of the map  $\mathbf{w}$  in equation (B.1) in the basis  $\Sigma' = \{v'_{\sigma_1}, \dots, v'_{\sigma_{m-n+1}}\}$  for  $\text{Ker}'(B)$ .

### Appendix C. Proofs of results in Section 2.

#### C.1. Proof of Theorem 2.1.

*Proof.* Before we proceed with the proof, we state a useful observation. Consider the potential energy function

$$\mathcal{H}(\theta) = \sum_{(i,j) \in \mathcal{E}} a_{ij} H_e(\theta_i - \theta_j) = \sum_{(i,j) \in \mathcal{E}} a_{ij} H_e(d_{cc}(\theta_i, \theta_j))$$

We fix  $e = (i, j) \in \mathcal{E}$  and we show that  $H_e$  is differentiable at  $\theta$ . Note that  $H_e$  is twice differentiable. Since,  $\theta \in \mathbb{T}^n$  satisfies the angle constraint (1.1c), the counterclockwise difference  $d_{cc}$  is a differentiable function at  $\theta \in \mathbb{T}^n$ . This implies that  $H_e$  is differentiable at  $\theta$ . Let  $\Sigma$  be a cycle basis for graph  $G$ . Since  $\theta \in \mathbb{T}^n$  satisfies the angle constraint (1.1c), by Theorem 3.5(i), there exists  $\mathbf{u} \in \text{Img}(\mathbf{w}_\Sigma)$  such that  $\theta \in \Omega_{\mathbf{u}}^G$ . Now, using Theorem 3.6, there exists a bijection between  $[\theta] \in \Omega_{\mathbf{u}}^G / \mathbb{T}^1$  and  $\mathbf{x} \in P_{\mathbf{u}}$  such that  $(B^\top \theta) = B^\top \mathbf{x} + 2\pi C_\Sigma^\dagger \mathbf{u}$ , where the vector  $(B^\top \theta)$  is defined by equation (2.3). This implies that, for  $e = (i, j) \in \mathcal{E}$ ,

$$(C.1) \quad \frac{\partial}{\partial \theta_i} d_{cc}(\theta_i, \theta_j) = \frac{\partial}{\partial \theta_i} (B^\top \theta)_e = \frac{\partial}{\partial x_i} (B^\top \mathbf{x} + 2\pi C_\Sigma^\dagger \mathbf{u})_e = +1.$$

Therefore, for every  $i \in \{1, \dots, n\}$ ,

$$(C.2) \quad \begin{aligned} \frac{\partial \mathcal{H}}{\partial \theta_i} &= \sum_{(k,j) \in \mathcal{E}} a_{kj} \frac{\partial}{\partial \theta_i} H_e(d_{cc}(\theta_k, \theta_j)) = \sum_{(k,j) \in \mathcal{E}} a_{kj} \frac{dH_e}{d\alpha}(d_{cc}(\theta_k, \theta_j)) \frac{\partial}{\partial \theta_i} d_{cc}(\theta_k, \theta_j) \\ &= \sum_{j=1}^n a_{ij} h_e(d_{cc}(\theta_i, \theta_j)) = \sum_{j=1}^n a_{ij} h_e(\theta_i - \theta_j). \end{aligned}$$

where for the last equality, we used the fact that  $\frac{dH_e}{d\alpha}(\alpha) = h_e(\alpha)$ , for every  $e \in \mathcal{E}$ . Now we go back to the proof of the theorem.

Regarding (i)  $\implies$  (ii), if  $(f, \theta)$  is a solution to the flow network problem (1.3), then using (1.1a), for every  $i \in \{1, \dots, n\}$ ,

$$(p_{sd})_i = \sum_{j=1}^n f_{(i,j)} = \sum_{j=1}^n a_{ij} h_e(\theta_i - \theta_j).$$

Using the equality (C.2), we obtain  $p_{sd} = \nabla_\theta \mathcal{H}(\theta)$ . The constraint (1.3b) is the same as the constraint (1.1c). Therefore,  $\theta$  is a solution for the elastic network problem (1.3).

Regarding (ii)  $\implies$  (i), suppose  $\theta$  is a solution for the elastic network problem (1.1). For every  $e = (i, j) \in \mathcal{E}$ , define  $f_e$  by

$$f_e = a_{ij} h_e(\theta_i - \theta_j).$$

Then note that, for every  $i \in \{1, \dots, n\}$ ,

$$(Bf)_i = \sum_{j=1}^n f_{(i,j)} = \sum_{j=1}^n a_{ij} h_e(\theta_i - \theta_j) = \frac{\partial \mathcal{H}}{\partial \theta_i}(\theta) = (\nabla_\theta \mathcal{H}(\theta))_i = (p_{sd})_i,$$

where the second last equality is because of equation (C.2). The constraint (1.1c) is the same as the constraint (1.3b). Therefore,  $(f, \theta)$  is a solution for the flow network problem (1.1).  $\square$

### C.2. Proof of Theorem 2.2.

*Proof.* First note that since  $G$  is connected and acyclic, we have  $\text{Ker}(B^\top) = \{0_{n-1}\}$ . This implies that  $f = AB^\top L^\dagger p_{\text{sd}}$  is the unique solution of the flow balance equation (1.1a).

Regarding (i)  $\Rightarrow$  (ii), note that, for every  $e \in \mathcal{E}$ ,  $h_e$  is an odd monotone function and  $|(B^\top L^\dagger p_{\text{sd}})_e| \leq |h_e(\gamma)|$ . This implies that there exists a unique  $v \in \mathbb{R}^{n-1}$  with  $\|v\|_\infty \leq \gamma$  such that  $h_e(v_e) = (B^\top L^\dagger p_{\text{sd}})_e$ , for every  $e \in \mathcal{E}$ . Note that the graph  $G$  is connected and acyclic. We start from an arbitrary node  $i$  in  $G$  and assign an arbitrary phase angle  $\theta_i \in \mathbb{T}^1$  to the node  $i$ . Then, for every node  $j$  that is a neighbor of  $i$ , we assign  $\theta_j \in \mathbb{T}^1$  such that  $\theta_i - \theta_j = v_e$ , where  $e = (i, j) \in \mathcal{E}$ . Now, we can repeat this process for every neighbor of the node  $i$  and continue to assign the phase angles to the nodes of  $G$ . Since  $G$  is connected, using this procedure, one would eventually assign a phase angle to every node of the graph. Additionally, since  $G$  is acyclic, every node will get a unique phase angle. This implies that there exists a unique  $\theta \in \mathbb{T}^n$ , modulo rotations, such that

$$v_e = \theta_i - \theta_j, \quad \text{for all } e = (i, j) \in \mathcal{E}.$$

Thus,  $(f, \theta)$  is a solution for the flow network problem (1.1).

Regarding (ii)  $\Rightarrow$  (i), if  $(f, \theta)$  is a solution of the flow network problem (1.1), then we have  $f_e = a_{ij}h_e(\theta_i - \theta_j)$ , for every  $e = (i, j) \in \mathcal{E}$  and therefore,

$$|(B^\top L^\dagger p_{\text{sd}})_e| = |h_e(\theta_i - \theta_j)| \leq |h_e(\gamma)|, \quad \text{for all } e = (i, j) \in \mathcal{E},$$

where for the last inequality we used the fact that  $|\theta_i - \theta_j| \leq \gamma$ .  $\square$

**Appendix D. Proofs of results in Section 3.** It is worth mentioning that the proofs in this section are completely independent of the results in Section 2.1. Therefore, we use some of these results for proving Theorem 2.1.

#### D.1. Proof of Theorem 3.3.

*Proof.* We start by noting that, if  $\sigma$  is a cycle in graph  $G$  and  $\theta \in \mathbb{T}_0^n$ , then  $w_\sigma(\theta) = v_\sigma^\top(B^\top \theta)$ , where the vector  $(B^\top \theta)$  is defined in equation (2.3). Regarding part (i), we use induction to show that  $w_\sigma(\theta)$  is an integer. We start with  $n_\sigma = 3$ . Consider the 3-cycle  $\sigma = (1, 2, 3, 1)$ . Suppose that nodes 1, 2, 3 are contained in an arc of length less than or equal to  $\pi$  as shown in Figure 4 (left). Then we denote  $d_{cc}(\theta_1, \theta_2) = \alpha$  and  $d_{cc}(\theta_2, \theta_3) = \beta$ . It is then clear that  $\alpha + \beta < \pi$ . But the counterclockwise arc from node 3 to node 1 has length larger than  $\pi$ . As a result, by definition of the counterclockwise difference, we have  $d_{cc}(\theta_3) = -\alpha - \beta$ . This means that

$$w_\sigma(\theta) = d_{cc}(\theta_1, \theta_2) + d_{cc}(\theta_2, \theta_3) + d_{cc}(\theta_3, \theta_1) = \alpha + \beta - \alpha - \beta = 0.$$

Similar argument can be used to show that in Figure 4 (middle) and Figure 4 (right) the winding number of  $\sigma$  is +1 and -1, respectively. Now suppose that, for  $k \in \mathbb{Z}_{\geq 0}$ ,  $w_\eta(\theta)$  is an integer for every cycle  $\eta$  with  $n_\eta \leq k$ . We show that every cycle with length  $k+1$  has an integer winding number. Consider the cycle  $\sigma = (1, 2, \dots, k+1, 1)$ . Define the cycles  $\sigma' = (1, 2, 3, 1)$  and  $\sigma'' = (1, 3, \dots, k+1, 1)$ . Then a straightforward calculation shows that  $v_\sigma = v_{\sigma'} + v_{\sigma''}$ . As a result, we have

$$w_\sigma(\theta) = v_\sigma^\top(B^\top \theta) = v_{\sigma'}^\top(B^\top \theta) + v_{\sigma''}^\top(B^\top \theta) = w_{\sigma'}(\theta) + w_{\sigma''}(\theta).$$

Since both  $\sigma'$  and  $\sigma''$  has length less than or equal to  $k$ , we have  $w_{\sigma'}(\theta), w_{\sigma''}(\theta) \in \mathbb{Z}$ . This implies that  $w_\sigma(\theta) \in \mathbb{Z}$ .

Now suppose that  $\sigma = (1, \dots, n_\sigma)$ . Note that, for every  $\alpha, \beta \in \mathbb{T}^1$  such that  $|\alpha - \beta| \leq \gamma$  we have  $|d_{cc}(\alpha, \beta)| \leq \gamma$ . Thus

$$|w_\sigma(\theta)| = \frac{1}{2\pi} \left| \sum_{i=1}^{n_\sigma} d_{cc}(\theta_i, \theta_{i+1}) \right| \leq \frac{1}{2\pi} \sum_{i=1}^{n_\sigma} |d_{cc}(\theta_i, \theta_{i+1})| \leq \frac{1}{2\pi} n_\sigma \gamma(\theta).$$

Since  $w_\sigma(\theta)$  is an integer, we get  $|w_\sigma(\theta)| \leq \left\lfloor \frac{\gamma(\theta) n_\sigma}{2\pi} \right\rfloor$ . For the second inequality, note that  $|d_{cc}(\alpha, \beta)| < \pi$ . Thus

$$\frac{\gamma(\theta) n_\sigma}{2\pi} < \frac{n_\sigma}{2}.$$

This implies that  $\left\lfloor \frac{\gamma(\theta) n_\sigma}{2\pi} \right\rfloor < \frac{n_\sigma}{2}$ . Since  $\left\lfloor \frac{\gamma(\theta) n_\sigma}{2\pi} \right\rfloor$  is an integer, we have  $\left\lfloor \frac{\gamma(\theta) n_\sigma}{2\pi} \right\rfloor \leq \left\lfloor \frac{n_\sigma}{2} \right\rfloor - 1$ . Regarding part (ii), first note that part (i) implies  $|w_{\sigma_i}| \leq \left\lfloor \frac{n_\sigma}{2} \right\rfloor - 1$ , for every  $i \in \{1, \dots, m - n + 1\}$ . In turn, this implies that

$$\text{Img}(\mathbf{w}_\Sigma) \subseteq \left\{ [u_1, \dots, u_{m-n+1}]^\top \mid u_i \in \mathbb{Z}, |u_i| \leq \left\lfloor n_{\sigma_i}/2 \right\rfloor - 1, \text{ for } i \in \{1, \dots, m - n + 1\} \right\},$$

and therefore the winding map  $\mathbf{w}_\Sigma$  has a finite range. Moreover, the counterclockwise angle difference map  $d_{cc} : \mathbb{T} \rightarrow [-\pi, \pi)$  is piecewise continuous on  $\mathbb{T}$ . Thus  $\mathbf{w}_\Sigma : \mathbb{T}_0^n \rightarrow \mathbb{Z}^{m-n+1}$  is a piecewise continuous map with a finite range. Therefore, the winding map  $\mathbf{w}_\Sigma$  is piecewise constant and this completes the proof of part (ii).  $\square$

### D.2. Proof of Theorem 3.5.

*Proof.* Regarding part (i), it is clear that, for every  $\mathbf{u} \in \text{Img}(\mathbf{w}_\Sigma)$ , we have  $\Omega_{\mathbf{u}}^G \subset \mathbb{T}_0^n$ . This implies that  $\bigcup_{\mathbf{u} \in \text{Img}(\mathbf{w}_\Sigma)} \Omega_{\mathbf{u}}^G \subseteq \mathbb{T}_0^n$ . Moreover, for every  $\theta \in \mathbb{T}_0^n$ , we have  $\theta \in \Omega_{\mathbf{w}_\Sigma(\theta)}^G$ . Therefore, we have  $\bigcup_{\mathbf{u} \in \text{Img}(\mathbf{w}_\Sigma)} \Omega_{\mathbf{u}}^G = \mathbb{T}_0^n$ . Finally, by taking closure of both side of this equality and noting that  $\text{closure}(\mathbb{T}_0^n) = \mathbb{T}^n$ , we get

$$\bigcup_{\mathbf{u} \in \text{Img}(\mathbf{w}_\Sigma)} \text{closure}(\Omega_{\mathbf{u}}^G) = \mathbb{T}^n.$$

Regarding part (ii), suppose that for some  $\mathbf{u} \neq \mathbf{v}$ , we have  $\theta \in \Omega_{\mathbf{u}}^G \cap \Omega_{\mathbf{v}}^G$ . Then,  $\mathbf{w}_\Sigma(\theta) = \mathbf{u} = \mathbf{v}$ , which is a contradiction. Therefore, we have  $\Omega_{\mathbf{u}}^G \cap \Omega_{\mathbf{v}}^G = \emptyset$ .  $\square$

### D.3. Proof of Theorem 3.6.

*Proof.* Regarding part (i), fix  $\theta \in \Omega_{\mathbf{u}}^G$ . By definition of the winding number, it is easy to see that, for every cycle  $\sigma$ , we have  $w_\sigma(\theta) = \frac{1}{2\pi} v_\sigma^\top (B^\top \theta)$ , where the vector  $(B^\top \theta)$  is defined in equation (2.3). Applying this formula to every cycle in the cycle basis  $\Sigma$ , we get  $\mathbf{u} = \mathbf{w}_\Sigma(\theta) = \frac{1}{2\pi} C_\Sigma (B^\top \theta)$ . Multiplying both side of this equality by  $C_\Sigma^\dagger$ , we get  $2\pi C_\Sigma^\dagger \mathbf{u} = C_\Sigma^\dagger C_\Sigma (B^\top \theta)$ . Note that, by properties of the Moore–Penrose inverse, we have  $C_\Sigma^\dagger C_\Sigma C_\Sigma^\dagger = C_\Sigma^\dagger$ . This implies that

$$(D.1) \quad C_\Sigma^\dagger C_\Sigma ((B^\top \theta) - 2\pi C_\Sigma^\dagger \mathbf{u}) = \mathbb{0}_m$$

On the other hand, by properties of the Moore–Penrose inverse, we have  $C_\Sigma C_\Sigma^\dagger C_\Sigma = C_\Sigma$ . Now suppose that  $\alpha \in \text{Ker}(C_\Sigma^\dagger C_\Sigma)$ . This means that  $C_\Sigma^\dagger C_\Sigma \alpha = \mathbb{0}_m$ . Multiplying both side of this equality by  $C_\Sigma$ , we get  $C_\Sigma \alpha = \mathbb{0}_m$ . This implies that  $\alpha \in \text{Ker}(C_\Sigma)$ . Therefore, we can deduce that  $\text{Ker}(C_\Sigma^\dagger C_\Sigma) \subseteq \text{Ker}(C_\Sigma)$ . Moreover it is easy to show that  $\text{Ker}(C_\Sigma) \subseteq \text{Ker}(C_\Sigma^\dagger C_\Sigma)$ . Therefore, we get  $\text{Ker}(C_\Sigma) = \text{Ker}(C_\Sigma^\dagger C_\Sigma)$ . In turn,

by Lemma A.1(ii), we have  $\text{Ker}(C_\Sigma) = \text{Img}(B^\top)$ . This implies that  $\text{Ker}(C_\Sigma^\dagger C_\Sigma) = \text{Img}(B^\top)$  and thus, using the equation (D.1), there exists a unique  $\mathbf{x} \in \mathbb{1}_n^\perp$  such that  $(B^\top \theta) - 2\pi C_\Sigma^\dagger \mathbf{u} = B^\top \mathbf{x}$ . In other words, there exists  $x \in \mathbb{1}_n^\perp$  such that  $(B^\top \theta) = B^\top \mathbf{x} + 2\pi C_\Sigma^\dagger \mathbf{u}$ . This completes the proof of (i). Regarding part (ii), we define the map  $\iota : \Omega_{\mathbf{u}}^G/\mathbb{T}^1 \rightarrow P_{\mathbf{u}}$  by  $\iota([\theta]) = \mathbf{x}$ , where  $\mathbf{x} \in \mathbb{1}_n^\perp$  is such that  $(B^\top \theta) = B^\top \mathbf{x} + 2\pi C_\Sigma^\dagger \mathbf{u}$ . We show that  $\iota$  is a bijection between  $\Omega_{\mathbf{u}}^G/\mathbb{T}^1$  and  $P_{\mathbf{u}}$ . Consider the linear equations

$$(D.2) \quad C_\Sigma \mathbf{z} = \mathbf{u}.$$

By Lemma A.1(iii), the system of linear equations (D.2) has an integer solution  $\mathbf{z}$ . By Lemma A.1(i), the matrix  $C_\Sigma$  is of rank  $m - n + 1$  and thus it has linearly independent rows. This implies that  $C_\Sigma C_\Sigma^\dagger = I_{m-n+1}$ . Therefore, we have  $C_\Sigma C_\Sigma^\dagger \mathbf{u} = \mathbf{u}$  and in turn  $C_\Sigma^\dagger \mathbf{u}$  is another solution for (D.2). Since both  $\mathbf{z}$  and  $C_\Sigma^\dagger \mathbf{u}$  are solutions for (D.2), we have  $\mathbf{z} - C_\Sigma^\dagger \mathbf{u} \in \text{Ker}(C_\Sigma)$ . Using Theorem A.1(ii), we have  $\text{Ker}(C_\Sigma) = \text{Img}(B^\top)$  and there exists  $\alpha \in \mathbb{1}_n^\perp$  such that  $\mathbf{z} - C_\Sigma^\dagger \mathbf{u} = B^\top \alpha$ . Now, we define the open set  $D = \{\mathbf{x} \in \mathbb{1}_n^\perp \mid \|B^\top \mathbf{x} + 2\pi C_\Sigma^\dagger \mathbf{u}\|_\infty < \pi\}$ . We first show that the map  $\iota$  is injective. Suppose that  $[\theta_1], [\theta_2] \in \Omega_{\mathbf{u}}^G/\mathbb{T}^1$  are such that  $\iota([\theta_1]) = \iota([\theta_2]) = \mathbf{x}$ . This implies that  $(B^\top \theta_1) = (B^\top \theta_2) = B^\top \mathbf{x} + 2\pi C_\Sigma^\dagger \mathbf{u}$  and as a result, we get  $\theta_1 = \text{rot}_s(\theta_2)$ , for some  $s \in [-\pi, \pi)$ . This completes the proof of the fact that  $\iota$  is injective. Now we show that  $\iota$  is surjective. Let  $\mathbf{x} \in D$ . Then we define  $\theta \in \mathbb{T}^1$  by

$$\theta = \text{mod}(\mathbf{x} - 2\pi\alpha, 2\pi).$$

Suppose that  $e = (i, j) \in \mathcal{E}$ . Then we have

$$(B^\top \theta)_e = d_{cc}(\theta_i, \theta_j) = (x_i - 2\pi\alpha_i) - (x_j - 2\pi\alpha_j) + 2\pi z_i,$$

where the second equality is because of the fact that

$$|(x_i - 2\pi\alpha_i) - (x_j - 2\pi\alpha_j) + 2\pi z_i| \leq \|B^\top \mathbf{x} - 2\pi\alpha + 2\pi\mathbf{z}\|_\infty = \|B^\top \mathbf{x} + 2\pi C_\Sigma^\dagger \mathbf{u}\|_\infty < \pi.$$

Therefore, we have  $(B^\top \theta) = B^\top (\mathbf{x} - 2\pi\alpha) + 2\pi\mathbf{z} = B^\top \mathbf{x} + 2\pi C_\Sigma^\dagger \mathbf{u}$ . This implies that  $\iota([\theta]) = \mathbf{x}$  and completes the proof of bijection of  $\iota$ . Now we show that  $\iota : \Omega_{\mathbf{u}}^G/\mathbb{T}^1 \rightarrow P_{\mathbf{u}}$  is a continuous map. Let us define the map  $\xi : \Omega_{\mathbf{u}}^G \rightarrow P_{\mathbf{u}}$  by  $\xi(\theta) = \iota([\theta])$ , for every  $\theta \in \Omega_{\mathbf{u}}^G$ . Then, by [55, Theorem 22.2], the map  $\iota$  is continuous if and only if the map  $\xi$  is continuous. Suppose that  $\phi, \psi \in \Omega_{\mathbf{u}}^G$  and  $y = \iota([\phi])$  and  $z = \iota([\psi])$ . Note that, the graph  $G$  is connected. Thus, by [7, Lemma 6.12(iii)], we have  $(BB^\top)^\dagger BB^\top = I_n - \frac{1}{n} \mathbb{1}_n \mathbb{1}_n^\top$ . As a result, we have

$$(D.3) \quad \|y - z\| \leq \|(BB^\top)^\dagger B\| \|B^\top y - B^\top z\| = \|(BB^\top)^\dagger B\| \|(B^\top \phi) - (B^\top \psi)\|. \quad \square$$

On the other hand, since  $\iota$  is a bijection, we have  $\|(B^\top \theta)\|_\infty < \pi$ , for every  $\theta \in \Omega_{\mathbf{u}}^G$ . As a result, the map  $\theta \mapsto (B^\top \theta)$  is continuous on  $\Omega_{\mathbf{u}}^G$ . This together with the inequality (D.3) imply that the map  $\xi : \theta \mapsto x$  is continuous and thus  $\iota$  is continuous. Moreover,  $P_{\mathbf{u}}$  is a Hausdorff space. Therefore, by [55, Theorem 26.6], the map  $\iota$  is a homeomorphism on any compact subset of  $\Omega_{\mathbf{u}}^G/\mathbb{T}^1$ .

## Appendix E. Proofs of results in Section 4.

### E.1. Proof of Theorem 4.1.

*Proof.* Suppose that  $(f, \phi)$  and  $(g, \psi)$  are two solutions for the flow network problem (1.1) with  $\mathbf{w}_\Sigma(\phi) = \mathbf{w}_\Sigma(\psi) = \mathbf{u}$ . Then, by Theorem 5.1,  $f$  and  $g$  satisfies the  $\mathbf{u}$  winding balance equation (5.1). Thus, we have  $f, g \in F_{\text{sd}}$  and

$$T_{\mathbf{u}}(f) = f - L_{\min} \mathcal{P}_{L_{\min}}(h_\gamma^{-1}(\mathcal{A}^{-1}f) - 2\pi C_\Sigma^\dagger \mathbf{u}) = f$$

where the last equality holds because  $f$  satisfies (5.1a). Similarly, one can show that  $T_{\mathbf{u}}(g) = g$ . Thus, by Theorem 5.2(i), we get  $f = g$ . By the equivalence of parts (iii) and (iv) in Theorem 5.2, we get that  $\phi = \psi$ . As a result, there should exists at most one solution for the flow network problem 1.1 with the phase angle in the winding cell  $\Omega_{\mathbf{u}}^G$ .  $\square$

### E.2. Proof of Corollary 4.2.

*Proof.* Regarding part (i), the result is already proved in Theorem 4.1. Regarding part (ii), suppose that  $(f, \theta)$  is a solution of the flow network problem (1.1) such that  $\theta \in \Omega_{\mathbf{u}}^G$ . Then, for every  $\sigma \in \Sigma$ ,

$$|w_\sigma(\theta)| = \frac{1}{2\pi} \left| \sum_{i=1}^{n_\sigma} d_{\text{cc}}(\theta_i, \theta_{i+1}) \right| \leq \frac{1}{2\pi} \sum_{i=1}^{n_\sigma} |d_{\text{cc}}(\theta_i, \theta_{i+1})| \leq \frac{1}{2\pi} n_\sigma \gamma,$$

where for the last equality we used  $|d_{\text{cc}}(\theta_i, \theta_{i+1})| = |\theta_i - \theta_j| \leq \gamma$ . Since  $w_\sigma(\theta)$  is an integer, we get

$$(E.1) \quad |w_\sigma(\theta)| \leq \left\lfloor \frac{n_\sigma \gamma}{2\pi} \right\rfloor.$$

Moreover, we know that  $n_\sigma \leq k$ . This implies that  $|w_\sigma(\theta)| \leq \frac{1}{2\pi} \gamma k$ . As a result, we should have  $\|\mathbf{u}\|_\infty \leq \left\lfloor \frac{k\gamma}{2\pi} \right\rfloor$ . This implies that, if  $\|\mathbf{u}\|_\infty > \left\lfloor \frac{k\gamma}{2\pi} \right\rfloor$ , we have  $\mathbf{u} \notin \text{Img}(\mathbf{w}_\Sigma)$  and thus there is no solution  $(f, \theta)$  for the flow network problem (1.1) such that  $\theta \in \Omega_{\mathbf{u}}^G$ . Regarding part (iii), using the inequality (E.1), we get  $\text{Img}(\mathbf{w}_\Sigma) \leq \prod_{i=1}^{m-n+1} |w_\sigma(\theta)| \leq \prod_{i=1}^{m-n+1} \left\lfloor \frac{n_{\sigma_i} \gamma}{2\pi} \right\rfloor$ .  $\square$

### E.3. Proof of Theorem 4.3.

*Proof.* Recall that, for  $\theta \in \mathbb{T}^n$ , the vector  $(B^\top \theta)$  is defined by equation (2.3). Regarding part (ii), note that  $\text{Img}(\mathcal{A}B^\top) \oplus \text{Ker}(B) = \mathbb{R}^m$ . Therefore, there exists a unique decomposition  $f = f^{\text{cut}} + f^{\text{cyc}}$ , where  $f^{\text{cut}} \in \text{Img}(\mathcal{A}B^\top)$  and  $f^{\text{cyc}} \in \text{Ker}(B)$ . Additionally, the edge vector  $f \in \mathbb{R}^m$  satisfies the flow balance equation (1.1a), that is  $Bf = p_{\text{sd}}$ . Note that  $f^{\text{cyc}} \in \text{Ker}(B)$  and this implies that  $Bf^{\text{cut}} = p_{\text{sd}}$ . Moreover,  $f_{\text{cut}} \in \text{Img}(\mathcal{A}B^\top)$  and therefore there exists  $x \in \mathbb{1}_n^\perp$  such that  $f^{\text{cut}} = \mathcal{A}B^\top x$ . This implies that  $B\mathcal{A}B^\top x = Lx = p_{\text{sd}}$ . Finally, one can compute  $f^{\text{cut}} = \mathcal{A}B^\top x = \mathcal{A}B^\top L^\dagger p_{\text{sd}}$ . This completes the proof of part (ii). Regarding part (iii), note that, we have  $p_{\text{sd}} = Bf = Bg$ . This implies that  $B(f - g) = 0$  and in turn  $f - g \in \text{Ker}(B)$ . Regarding part (iv), given  $\phi = \psi$ , it is trivial to see that  $f = g$ . Now suppose that, for  $\phi, \psi$ , we have  $f = g$ . This implies that, for every  $e = (i, j) \in \mathcal{E}$ , we have  $h_e(\phi_i - \phi_j) = h_e(\psi_i - \psi_j)$ . Since  $h_e$  is monotone on the interval  $[-\gamma, \gamma]$ , it is invertible on this interval. This implies that  $\phi_i - \phi_j = \psi_i - \psi_j$ , for every  $(i, j) \in \mathcal{E}$ . This means that  $(B^\top \phi) = (B^\top \psi)$ . By Theorem 3.6(i), there exists  $\mathbf{x}, \mathbf{y} \in \mathbb{1}_n^\perp$  such that

$$\begin{aligned} (B^\top \phi) &= B^\top \mathbf{x} + 2\pi C_\Sigma^\dagger(\mathbf{w}_\Sigma(\phi)), \\ (B^\top \psi) &= B^\top \mathbf{y} + 2\pi C_\Sigma^\dagger(\mathbf{w}_\Sigma(\psi)) \end{aligned}$$

We multiply both side of the above equations by  $C_\Sigma$ . Note that, by Lemma A.1(ii) we have  $\text{Ker}(C_\Sigma) = \text{Img}(B^\top)$ . This implies that

$$C_\Sigma C_\Sigma^\dagger (\mathbf{w}_\Sigma(\psi) - \mathbf{w}_\Sigma(\phi)) = \mathbf{0}_{m-n+1}.$$

By Lemma A.1(i), the matrix  $C_\Sigma$  is of rank  $m - n + 1$  and therefore  $C_\Sigma$  has linearly independent rows. Thus,  $C_\Sigma C_\Sigma^\dagger = I_{m-n+1}$  and this implies that  $\mathbf{w}_\Sigma(\psi) = \mathbf{w}_\Sigma(\phi)$ . Now suppose that  $\mathbf{w}_\Sigma(\psi) = \mathbf{w}_\Sigma(\phi)$ , the  $(f, \phi)$  and  $(g, \psi)$  are two solutions for the flow network problem (1.1) with the property that  $\phi, \psi \in \Omega_{\mathbf{u}}^G$ . Thus, by Theorem (4.1), we have  $f = g$  and  $\phi = \psi$  modulo rotations. Finally, if  $\phi = \text{rot}_s(\psi)$  for some  $s \in [-\pi, \pi)$ , then by equation (1.1b), it is clear that  $f = g$ . Regarding part (v), we start by introducing the function  $h: \mathbb{R}^m \rightarrow \mathbb{R}^m$  defined by

$$(h(y))_e = h_e(y_e), \quad \text{for every } e \in \mathcal{E}.$$

By the angle constraint (1.1c), for every  $e \in \mathcal{E}$ , we have  $|\theta_i - \theta_j| \leq \gamma$  and  $|\psi_i - \psi_j| \leq \gamma$ . Note also that, for every  $e \in \mathcal{E}$ , the flow  $h_e$  is a strictly increasing on the interval  $[-\gamma, \gamma]$ . This implies that

$$a_{ij} ((\phi_i - \phi_j) - (\psi_i - \psi_j)) (h_e(\phi_i - \phi_j) - h_e(\psi_i - \psi_j)) \geq 0.$$

Summing the above equation over all  $e = (i, j) \in \mathcal{E}$ , we get

$$(E.2) \quad (B^\top \phi - B^\top \psi)^\top \mathcal{A} (h(B^\top \phi) - h(B^\top \psi)) \geq 0.$$

Moreover, by Theorem 3.5(i), there exists  $\mathbf{x}, \mathbf{x}' \in \mathbb{1}_n^\perp$  such that

$$(E.3) \quad (B^\top \phi) = B^\top \mathbf{x} + 2\pi C_\Sigma^\dagger w_\sigma(\phi), \quad (B^\top \psi) = B^\top \mathbf{x}' + 2\pi C_\Sigma^\dagger w_\sigma(\psi).$$

Replacing (E.3) into (E.2), we get

$$(E.4) \quad \begin{aligned} & ((B^\top \phi) - (B^\top \psi))^\top \mathcal{A} (h(B^\top \phi) - h(B^\top \psi)) \\ &= (B^\top (\mathbf{x} - \mathbf{x}') + 2\pi C_\Sigma^\dagger (w_\sigma(\phi) - w_\sigma(\psi)))^\top \mathcal{A} (h(B^\top \phi) - h(B^\top \psi)) \\ &= (B^\top (\mathbf{x} - \mathbf{x}'))^\top \mathcal{A} (h(B^\top \phi) - h(B^\top \psi)) \end{aligned}$$

$$(E.5) \quad + (2\pi C_\Sigma^\dagger (w_\sigma(\phi) - w_\sigma(\psi)))^\top \mathcal{A} (h(B^\top \phi) - h(B^\top \psi)).$$

Note that the term (E.4) is

$$(B^\top (\mathbf{x} - \mathbf{x}'))^\top \mathcal{A} (h(B^\top \phi) - h(B^\top \psi)) = (\mathbf{x} - \mathbf{x}')^\top B \mathcal{A} (h(B^\top \phi) - h(B^\top \psi)).$$

Since  $(f, \phi)$  and  $(g, \psi)$  are solutions for the flow network problem (1.1), we get

$$B \mathcal{A} (h(B^\top \phi) - h(B^\top \psi)) = B(f - g) = p_{\text{sd}} - p_{\text{sd}} = \mathbf{0}_n.$$

Therefore, the term (E.4) is equal to zero. Moreover, since  $\sigma$  is the only cycle for  $G$ , we have  $C_\Sigma^\dagger = \frac{1}{n} v_\sigma$ . Therefore, the term (E.5) can be written as

$$\begin{aligned} & (2\pi C_\Sigma^\dagger (w_\sigma(\phi) - w_\sigma(\psi)))^\top \mathcal{A} (h(B^\top \phi) - h(B^\top \psi)) \\ &= \frac{1}{n} (w_\sigma(\phi) - w_\sigma(\psi)) v_\sigma^\top \mathcal{A} (h(B^\top \phi) - h(B^\top \psi)) \\ &= \frac{1}{n} (w_\sigma(\phi) - w_\sigma(\psi)) (v_\sigma^\top f - v_\sigma^\top g). \end{aligned}$$

Therefore, the inequality (E.2) can be written as  $\frac{1}{n} (w_\sigma(\phi) - w_\sigma(\psi)) (v_\sigma^\top f - v_\sigma^\top g) \geq 0$ . This completes the proof of part (v).  $\square$

**Appendix F. Proofs of results in Section 5.** It is worth mentioning that the proofs in this section are independent of the results in Section 4. Therefore, we use some of the results in this section to prove Theorem 4.1.

### F.1. Proof of Theorem 5.1.

*Proof.* Recall that, for  $\theta \in \mathbb{T}^n$ , the vector  $(B^\top \theta)$  is defined by equation (2.3). Regarding (i)  $\implies$  (ii), Suppose that  $(f, \theta)$  is a solution of flow network problem (1.1) with the property that  $\theta \in \Omega_{\mathbf{u}}^G$ . First note, for every  $e = (i, j) \in \mathcal{E}$ , we have  $f_e = a_{ij}h_e(\theta_i - \theta_j)$  and thus  $a_{ij}^{-1}f_e = h_e(\theta_i - \theta_j)$ . Using the angle constraint (1.1c), we have  $|\theta_i - \theta_j| \in [-\gamma, \gamma]$ , for every  $e = (i, j) \in \mathcal{E}$ . This implies that

$$(F.1) \quad |f_e| \leq a_{ij}|h_e(\gamma)|, \quad \text{for } e = (i, j) \in \mathcal{E}.$$

On the other hand, for every  $y \in [-\gamma, \gamma]$  and every  $e = (i, j) \in \mathcal{E}$ , we have  $h_e(y) = (h_\gamma)_e(y)$ . This means that  $f_e = a_{ij}h_e(\theta_i - \theta_j) = a_{ij}(h_\gamma)_e(\theta_i - \theta_j)$ . Since  $(h_\gamma)_e$  is monotone on  $\mathbb{R}$ , it is invertible and  $\theta_i - \theta_j = (h_\gamma)_e^{-1}(a_{ij}^{-1}f_e)$ . In the vector form, we get

$$(F.2) \quad (B^\top \theta) = h_\gamma^{-1}(\mathcal{A}^{-1}f).$$

Using Theorem 3.6(i), there exists  $\mathbf{x} \in \mathbb{1}_n^\perp$  such that  $(B^\top \theta) = B^\top \mathbf{x} + 2\pi C_\Sigma^\dagger \mathbf{u}$ . Plugging in the equation (F.2), we get

$$(F.3) \quad h_\gamma^{-1}(\mathcal{A}^{-1}f) - 2\pi C_\Sigma^\dagger \mathbf{u} = B^\top \mathbf{x}.$$

Multiplying both side of equation (F.3) by  $\mathcal{P}_{L_{\min}}$  and noting the fact that  $\mathcal{P}_{L_{\min}} L_{\min} \mathcal{A} B^\top \alpha = 0_m$ , we get

$$(F.4) \quad \mathcal{P}_{L_{\min}} L_{\min} \mathcal{A} (h_\gamma^{-1}(\mathcal{A}^{-1}f) - 2\pi C_\Sigma^\dagger \mathbf{u}) = 0_m.$$

Combining inequality (F.1) with the equality (F.4), we deduce that  $f$  is a solution of the  $\mathbf{u}$ -winding balance equation (5.1). Regarding (ii)  $\implies$  (i), suppose that  $f \in \mathbb{R}^m$  is a solution for the  $\mathbf{u}$ -winding balance equation (5.1). Note that  $\text{Ker}(\mathcal{P}_{L_{\min}} L_{\min} \mathcal{A}) = \text{Im}(B^\top)$ . Thus, by equality (5.1b), there exists  $\mathbf{x} \in \mathbb{1}_n^\perp$  such that

$$h_\gamma^{-1}(\mathcal{A}^{-1}f) = B^\top \mathbf{x} + 2\pi C_\Sigma^\dagger \mathbf{u}.$$

Note that, by the constraint (5.1c), for every  $e = (i, j) \in \mathcal{E}$ , we have

$$|a_{ij}f_e| \leq |h_e(\gamma)| = \max_{y \in [-\gamma, \gamma]} h_e(y).$$

Since, for each  $e \in \mathcal{E}$ ,  $(h_\gamma)_e$  is monotone on  $\mathbb{R}$  and  $(h_\gamma)_e(y) = h_e(y)$ , for every  $y \in [-\gamma, \gamma]$ , we get that  $\|h_\gamma^{-1}(\mathcal{A}^{-1}f)\|_\infty \leq \gamma$ . As a result, we have

$$(F.5) \quad \|B^\top \mathbf{x} + 2\pi C_\Sigma^\dagger \mathbf{u}\|_\infty \leq \gamma$$

This means that  $\mathbf{x} \in P_{\mathbf{u}}$ . Now, by Theorem 3.6(ii) there exists  $\theta \in \Omega_{\mathbf{u}}^G$  such that  $(B^\top \theta) = B^\top \mathbf{x} + 2\pi C_\Sigma^\dagger \mathbf{u}$  and thus  $h_\gamma^{-1}(\mathcal{A}^{-1}f) = (B^\top \theta)$ . On the other hand, for every  $y \in [-\gamma, \gamma]$  and every  $e = (i, j) \in \mathcal{E}$ , we have  $h_e(y) = (h_\gamma)_e(y)$ . As a result, for every  $e = (i, j) \in \mathcal{E}$ ,

$$(F.6) \quad f_e = a_{ij}h_e(\theta_i - \theta_j).$$



Moreover, the inequality (F.5) implies that

$$(F.7) \quad |\theta_i - \theta_j| \leq \gamma.$$

The equations (F.6), (5.1a), and (F.7) imply that  $(f, \theta)$  is a solution for the flow network problem. Finally, we show that  $\theta$  is the unique phase angle vector in  $\Omega_{\mathbf{u}}^G$  for which  $(f, \theta)$  is a solution of flow network problem (1.1). Suppose that  $(f, \phi)$  is another solution for flow network problem (1.1) with  $\phi \in \Omega_{\mathbf{u}}^G$ . For every  $e = (i, j) \in \mathcal{E}$ , we have  $f_e = a_{ij}h_e(\theta_i - \theta_j) = a_{ij}h_e(\phi_i - \phi_j)$ . Moreover,  $|\theta_i - \theta_j| \leq \gamma$  and  $|\phi_i - \phi_j| \leq \gamma$  and  $h_e$  is monotone on  $[-\gamma, \gamma]$ . This implies that  $\theta_i - \theta_j = \phi_i - \phi_j$ , for every  $(i, j) \in \mathcal{E}$ . In the vector form, this leads to  $(B^\top \theta) = (B^\top \phi)$ . Note that  $\theta, \phi \in \Omega_{\mathbf{u}}^G$ . Thus, there exists  $\mathbf{x}, \mathbf{y} \in P_{\mathbf{u}}$  such that the bijection in Theorem 3.6(ii) maps  $\theta$  to  $\mathbf{x}$  and maps  $\phi$  to  $\mathbf{y}$ . Using Theorem 3.6(i), we get

$$(B^\top \theta) = B^\top \mathbf{x} + 2\pi C_\Sigma^\dagger \mathbf{u}, \quad (B^\top \phi) = B^\top \mathbf{y} + 2\pi C_\Sigma^\dagger \mathbf{u}.$$

Since  $(B^\top \theta) = (B^\top \phi)$ , we get that  $B^\top (\mathbf{x} - \mathbf{y}) = \mathbf{0}_m$ . Since  $G$  is strongly connected,  $\text{Ker}(B^\top) = \text{span}\{\mathbf{1}_n\}$ . Since both  $\mathbf{x}$  and  $\mathbf{y}$  are in  $\mathbf{1}_n^\perp$ , this implies that  $\mathbf{x} = \mathbf{y}$  and as a result  $\theta = \phi$ , modulo rotations.  $\square$

## F.2. Proof of Theorem 5.2. .

*Proof.* Regarding parts (i) and (ii), note that, for every  $\eta_1, \eta_2 \in F_{\text{sd}}$ ,

$$T_{\mathbf{u}}(\eta_1) - T_{\mathbf{u}}(\eta_2) = \eta_1 - \eta_2 + \mathcal{P}_{L_{\min}} L_{\min} \mathcal{A} (h_\gamma^{-1}(\eta_1) - h_\gamma^{-1}(\eta_2)).$$

Since  $\eta_1, \eta_2 \in F_{\text{sd}}$ , we get  $\eta_1 - \eta_2 \in \text{Ker}(B)$ . This implies that  $\eta_1 - \eta_2 = \mathcal{P}_{L_{\min}} (\eta_1 - \eta_2)$ . As a result,

$$T_{\mathbf{u}}(\eta_1) - T_{\mathbf{u}}(\eta_2) = \mathcal{P}_{L_{\min}} (\eta_1 - \eta_2 - L_{\min} \mathcal{A} (h_\gamma^{-1}(\eta_1) - h_\gamma^{-1}(\eta_2))).$$

For the brevity of notation, we introduce the positive diagonal matrix  $D \in \mathbb{R}^{m \times m}$  by  $D = L_{\min} \mathcal{A}$ . By the Mean Value Inequality [1, Proposition 2.4.7],

$$\|T_{\mathbf{u}}(\eta_1) - T_{\mathbf{u}}(\eta_2)\|_D \leq \sup_{x \in \mathbb{R}^m} \|\mathcal{P}_{L_{\min}} (I_m - L_{\min} \nabla h_\gamma^{-1}(x))\|_D \|\eta_1 - \eta_2\|_D.$$

Using the fact that  $\|\mathbf{x}\|_D = \|D^{\frac{1}{2}} \mathbf{x}\|_2$ , we get

$$\|\mathcal{P}_{L_{\min}} (I_m - L_{\min} \nabla h_\gamma^{-1}(x))\|_D = \|D^{\frac{1}{2}} \mathcal{P}_{L_{\min}} (I_m - L_{\min} \nabla h_\gamma^{-1}(x)) D^{-\frac{1}{2}}\|_2.$$

Note that, by triangle inequality, we have

$$\begin{aligned} \|D^{\frac{1}{2}} \mathcal{P}_{L_{\min}} (I_m - L_{\min} \nabla h_\gamma^{-1}(x)) D^{-\frac{1}{2}}\|_2 &\leq \|D^{\frac{1}{2}} \mathcal{P}_{L_{\min}} D^{-\frac{1}{2}}\|_2 \|D^{\frac{1}{2}} (I_m - L_{\min} \nabla h_\gamma^{-1}(x)) D^{-\frac{1}{2}}\|_2 \\ &= \|D^{\frac{1}{2}} (I_m - L_{\min} \nabla h_\gamma^{-1}(x)) D^{-\frac{1}{2}}\|_2, \end{aligned} \quad \blacksquare$$

where in the last inequality we used the fact that  $D^{\frac{1}{2}} \mathcal{P}_{L_{\min}} D^{-\frac{1}{2}}$  is a symmetric idempotent matrix and therefore, its 2-norm is equal to 1. Moreover, for every  $x \in \mathbb{R}^m$ ,  $\nabla h_\gamma^{-1}(x)$  is a diagonal matrix such that, for every  $i \in \{1, \dots, m\}$ , we have

$$|(\nabla h_\gamma^{-1}(x))_{ii}| \leq (L_{\max}^{-1})_{ii}, \quad \text{for all } x \in \mathbb{R}^m$$

Additionally, by [26, Theorem 5.6.36], we have

$$\left\| D^{\frac{1}{2}} (I_m - L_{\min} \nabla h_{\gamma}^{-1}(x)) D^{-\frac{1}{2}} \right\|_2 = \|I_m - L_{\min} \nabla h_{\gamma}^{-1}(x)\|_{\infty} = \max_i \{ |1 - (L_{\min})_{ii} (\nabla h_{\gamma}^{-1}(x))_{ii}| \}.$$

Note that, for every  $x \in \mathbb{R}^m$  and every  $i \in \{1, \dots, m\}$ , we have

$$|1 - (L_{\min})_{ii} (\nabla h_{\gamma}^{-1}(x))_{ii}| \leq \|I_m - L_{\min} L_{\max}^{-1}\|_{\infty}.$$

This implies that

$$\sup_{x \in \mathbb{R}^m} \left\| D^{\frac{1}{2}} (I_m - L_{\min} \nabla h_{\gamma}^{-1}(x)) D^{-\frac{1}{2}} \right\|_2 = \sup_{x \in \mathbb{R}^m} \|I_m - L_{\min} \nabla h_{\gamma}^{-1}(x)\|_{\infty} \leq \|I_m - L_{\min} L_{\max}^{-1}\|_{\infty}.$$

As a result, we get

$$(F.8) \quad \|T_{\mathbf{u}}(\eta_1) - T_{\mathbf{u}}(\eta_2)\|_D \leq \|I_m - L_{\min} L_{\max}^{-1}\|_{\infty} \|\eta_1 - \eta_2\|_D.$$

Thus,  $T_{\mathbf{u}} : F_{\text{sd}} \rightarrow F_{\text{sd}}$  is a contraction mapping with respect to the norm  $\|\cdot\|_{\mathcal{A}}$  on the vector space  $F_{\text{sd}}$ . Therefore, by the Banach Fixed-point Theorem, there exists a unique  $f^* \in F_{\text{sd}}$  such that  $f^* = T_{\mathbf{u}}(f^*)$ . This completes the proof of part (i). Regarding part (ii), using the contraction property of  $T_{\mathbf{u}}$  in equation (F.8), for every  $k \in \mathbb{N}$ , we get

$$\|T_{\mathbf{u}}^{(k+1)}(f^{(0)}) - T_{\mathbf{u}}^{(k)}(f^{(0)})\|_D \leq \|I_m - L_{\min} L_{\max}^{-1}\|_{\infty} \|T_{\mathbf{u}}^{(k)}(f^{(0)}) - T_{\mathbf{u}}^{(k-1)}(f^{(0)})\|_D.$$

This implies that, for every  $k \in \mathbb{N}$ , we have

$$\|f^{(k+1)} - f^{(k)}\|_D \leq \|I_m - L_{\min} L_{\max}^{-1}\|_{\infty}^k \|T_{\mathbf{u}}(f^{(0)}) - f^{(0)}\|_D.$$

Now we show the equivalence of the statements (iii) and (iv).

(iii)  $\implies$  (iv): Since  $f_{\mathbf{u}}^*$  is the limit point of the converging sequence  $\{T_{\mathbf{u}}^k\}_{k \in \mathbb{N}}$ , we have  $T_{\mathbf{u}}(f_{\mathbf{u}}^*) = f_{\mathbf{u}}^*$ . Since  $L_{\min} \in \mathbb{R}^{m \times m}$  is an invertible diagonal matrix, we get

$$\mathcal{P}_{L_{\min}} L_{\min} \mathcal{A}(h_{\gamma}^{-1}(\mathcal{A}^{-1} f_{\mathbf{u}}^*) - 2\pi C_{\Sigma}^{\dagger} \mathbf{u}) = \mathbf{0}_m$$

Adding the condition that, for every  $e = (i, j) \in \mathcal{E}$ , we have  $|(f_{\mathbf{u}}^*)_e| \leq a_{ij} |h_e(\gamma)|$ , we deduce that  $f_{\mathbf{u}}^*$  satisfies  $\mathbf{u}$ -winding balance equation (5.1). Now we show that  $f_{\mathbf{u}}^*$  is the unique solution of the  $\mathbf{u}$ -winding balance equation (5.1). Suppose that there exists  $g \in \mathbb{R}^m$  such that  $g$  satisfies the  $\mathbf{u}$ -winding balance equation (5.1). In this case, by equation (5.1a), we have that  $g \in F_{\text{sd}}$  and

$$T_{\mathbf{u}}(g) = g - \mathcal{P}_{L_{\min}} L_{\min} \mathcal{A}(h_{\gamma}^{-1}(\mathcal{A}^{-1} g) - 2\pi C_{\Sigma}^{\dagger} \mathbf{u}) = g,$$

where the last equality holds because of (5.1b). As a result  $g$  is a fixed-point for the map  $T_{\mathbf{u}}$ . Thus, by part (i), we should have  $g = \lim_{k \rightarrow \infty} T_{\mathbf{u}}^k(g) = f_{\mathbf{u}}^*$ .

(iv)  $\implies$  (iii): Suppose that  $f_{\mathbf{u}}^*$  is a solution for the  $\mathbf{u}$ -winding balance equation (5.1). It should satisfies the flow constraint condition (5.1c). This implies that  $|(f_{\mathbf{u}}^*)_e| \leq a_{ij} |h_e(\gamma)|$ , for every  $e = (i, j) \in \mathcal{E}$ . Regarding (iv)  $\iff$  (v): the proof follows from Theorem 5.1. Moreover, if  $(f_{\mathbf{u}}^*, \theta^*)$  is the unique solution of the flow network problem (1.1) with  $\theta^* \in \Omega_{\mathbf{u}}^G$ , then, by the proof of Theorem 5.1, there exists  $\mathbf{x} \in \mathbb{1}_n^{\perp}$  such that  $B^{\top} \mathbf{x} + 2\pi C_{\Sigma}^{\dagger} \mathbf{u} = h_{\gamma}^{-1}(\mathcal{A} f_{\mathbf{u}}^*)$ . This implies that

$$\mathbf{x} = L^{\dagger} B \mathcal{A}(h_{\gamma}^{-1}(\mathcal{A}^{-1} f_{\mathbf{u}}^*) - 2\pi C_{\Sigma}^{\dagger} \mathbf{u}).$$

By Theorem 3.6(ii), we can identify  $\mathbf{x}$  and  $\theta^*$  and thus  $\theta^* = L^{\dagger} B \mathcal{A}(h_{\gamma}^{-1}(\mathcal{A}^{-1} f_{\mathbf{u}}^*) - 2\pi C_{\Sigma}^{\dagger} \mathbf{u})$ .  $\square$

**F.3. Proof of Theorem 5.4.** As a first step in the proof of Theorem 5.4, we prove the following useful lemma.

LEMMA F.1. *Consider an undirected weighted connected graph  $G$  with a cycle basis  $\Sigma$ . Then, for every  $\mathbf{u} \in \text{Im}(\mathbf{w}_\Sigma)$ , the system of linear equations*

$$(F.9) \quad C_\Sigma \mathbf{z} = \mathbf{u},$$

*can be solved in  $\mathcal{O}(nm)$ .*

*Proof.* Let  $\mathcal{T}$  be a spanning tree in  $G$  and, without loss of generality, assume that  $\mathcal{E} - \mathcal{E}_\mathcal{T} = \{e_1, \dots, e_{m-n+1}\}$ . Then, for every  $i \in \{1, \dots, m-n+1\}$ , we define the cycle  $\sigma'_i$  by  $\sigma'_i = (i_1, \dots, i_k, i_1)$ , where  $e_i = (i_1, i_k)$  and  $(i_1, \dots, i_k)$  is the unique simple path in the spanning tree  $\mathcal{T}$  between nodes  $i_1$  and  $i_k$ . Then one can easily show that  $\Sigma' = \{\sigma'_1, \dots, \sigma'_{m-n+1}\}$  is a cycle basis for  $G$ . Since  $\Sigma$  is also a cycle basis for  $G$ , there exists an invertible matrix  $R = \{r_{ij}\}$  such that

$$(F.10) \quad v_{\sigma'_i} = \sum_{j=1}^{m-n+1} r_{ji} v_{\sigma_j}$$

Moreover, each cycle in  $G$  has at most  $n$  edges, it is easy to check that, at most  $n$  entries in each rows of  $R$  are non-zero. Using equations (F.10), one can deduce that  $C_{\Sigma'} = RC_\Sigma$ . This implies that  $\mathbf{z}$  is a solution for equations (F.9) if and only if it is a solution for  $C_{\Sigma'} \mathbf{z} = R\mathbf{u}$ . Note that  $\mathbf{z} = [\mathbf{0}_{n-1}, R\mathbf{u}]^\top$  is a solution to  $C_{\Sigma'} \mathbf{z} = R\mathbf{u}$  and therefore a solution to equations (F.9). Thus, by computing  $R\mathbf{u}$ , one can find the solution to the linear systems of equations (F.9). Note  $R \in \mathbb{R}^{(m-n+1) \times (m-n+1)}$  and in each row of  $R$  there is at most  $n$  non-zero element. Thus, the computational complexity of finding  $R\mathbf{u}$  and finding a solution for (F.9) is  $\mathcal{O}(nm)$ .  $\square$

Now we go back to the proof of Theorem 5.4.

*Proof.* Regarding part (i), since we have  $|w_{\sigma_i}| \leq \lfloor \frac{\gamma n_{\sigma_i}}{2\pi} \rfloor$ , for every  $i \in \{1, \dots, m-n+1\}$ . Thus, the total number of times that the for-loop at step 2: is executed is  $\prod_{i=1}^{m-n+1} \lfloor \frac{\gamma n_{\sigma_i}}{2\pi} \rfloor$ . Regarding part (ii), the computational time of the iterations (5.3) to check for the existence and/or compute the solution of the flow network problem (1.1) is

$$(F.11) \quad (\text{Run time for each iterations}) \times (\text{the number of iterations}).$$

If  $\rho \in \mathbb{R}_{>0}$  is the tolerance of the numerical method, then, using Theorem 5.2(ii), the number of iterations is bounded above by

$$\frac{\log(\rho^{-1}) - \log\left(\|T_{\mathbf{u}}(f^{(0)}) - f^{(0)}\|_{L_{\min} \mathcal{A}}\right)}{\log(\|I_m - L_{\min} L_{\max}^{-1}\|_\infty)},$$

which is independent of  $n$  and  $m$ . Therefore, the number of iterations is  $\mathcal{O}(\rho^{-1})$ . Now we investigate the computational time for each iteration. For the iteration step  $k+1$ , we need to compute the terms  $f^{(k)}$ ,  $L_{\min} \mathcal{P}_{L_{\min}} h_\gamma^{-1}(\mathcal{A}^{-1} f^{(k)})$ , and  $L_{\min} \mathcal{P}_{L_{\min}} C_\Sigma^\dagger \mathbf{u}$  and then add them together. In what follows, we analyze the computational complexity of each of these terms.

- (i) The term  $f^{(k)}$  has already been computed from step  $k$ .
- (ii) Let  $D \in \mathbb{R}^m$  be a diagonal matrix. then, for every  $\eta \in \mathbb{R}^m$ , the computational time for  $D\eta$  is  $\mathcal{O}(m)$ .

- (iii) Note that the functions  $h_\gamma$  and  $h_\gamma^{-1}$  can be computed offline and therefore computing  $h_\gamma^{-1}(\mathcal{A}^{-1}f^{(k)})$  can be done in  $\mathcal{O}(m)$ .
- (iv) For every  $\eta \in \mathbb{R}^m$ , we have

$$\mathcal{P}_{L_{\min}} \eta = \eta - L_{\min} \mathcal{A} B^\top (B L_{\min} \mathcal{A} B^\top)^\dagger B \eta$$

In order to compute  $L_{\min} \mathcal{A} B^\top (B L_{\min} \mathcal{A} B^\top)^\dagger B \eta$ , we consider the following equality

$$B^\top (B L_{\min} \mathcal{A} B^\top)^\dagger B \eta = B^\top \mathbf{y},$$

where  $\mathbf{y}$  is the solution to the linear equations  $B L_{\min} \mathcal{A} B^\top \mathbf{y} = B \eta$ . Thus computing  $B^\top (B L_{\min} \mathcal{A} B^\top)^\dagger B \eta$  is equivalent to computing  $\mathbf{y}$  and then multiplying it by  $B^\top$ . Using the  $LU$  decomposition method, one can compute  $\mathbf{y}$  in  $\mathcal{O}(n^3)$  time [20, §3.2]. Moreover, each row in matrix  $B^\top$  has exactly 2 nonzero element. Thus, given  $\mathbf{y}$ , the term  $B^\top \mathbf{y}$  can be computed in  $\mathcal{O}(n)$  in time. Therefore, the computational time for computing the term  $\mathcal{P}_{L_{\min}} \eta$  is in  $\mathcal{O}(n^3)$  in time.

- (v) By parts (ii), (iii), and (iv), the computational time for the term  $\mathcal{P}_{L_{\min}} L_{\min} \mathcal{A} h_\gamma^{-1}(\mathcal{A}^{-1}f^{(k)})$  is  $\mathcal{O}(n^3)$ .
- (vi) Since  $\text{Ker}(C_\Sigma) = \text{Im}(B^\top) = \text{Ker}(\mathcal{P}_{L_{\min}} L_{\min} \mathcal{A})$ , then we have

$$2\pi \mathcal{P}_{L_{\min}} L_{\min} \mathcal{A} C_\Sigma^\dagger \mathbf{u} = 2\pi \mathcal{P}_{L_{\min}} L_{\min} \mathcal{A} \mathbf{z},$$

where  $\mathbf{z}$  is the solution of the linear system of equations  $C_\Sigma \mathbf{z} = \mathbf{u}$ . By Lemma F.1,  $\mathbf{z}$  can be computed in  $\mathcal{O}(mn)$ . By parts (ii), (iii), and (iv),  $2\pi \mathcal{P}_{L_{\min}} L_{\min} \mathcal{A} \mathbf{z}$  can be computed in  $\mathcal{O}(n^3)$ .

Therefore, each iteration of the projection iteration can be computed in at most  $\mathcal{O}(n^3)$  and, by equation (F.11), the projection iteration (5.3) can check the existence/compute the solutions of the flow network problem (1.1) in  $\mathcal{O}(n^3) \times \mathcal{O}(\log(\rho^{-1})) = \mathcal{O}(\log(\rho^{-1})n^3)$  time. Regarding part (iii), note that the run time of the for-loop in steps 2-11: is given by

$$(F.12) \quad (\text{Run time for one execution of for-loop}) \times (\text{the number of for-loops}).$$

By part (i), the run time for one execution of the for-loop is  $\mathcal{O}(\log(\rho^{-1})n^3)$ . Also, by part (ii), the number of time the for-loop is invoked is  $\prod_{i=1}^{m-n+1} \left\lfloor \frac{\gamma n_{\sigma_i}}{2\pi} \right\rfloor$ . This means that the run time for in steps 2-11: is

$$\mathcal{O}(\log(\rho^{-1})n^3) \mathcal{O}\left(\prod_{i=1}^{m-n+1} \left\lfloor \frac{\gamma n_{\sigma_i}}{2\pi} \right\rfloor\right) = \mathcal{O}\left(\log(\rho^{-1})n^3 \left(\frac{\gamma}{2\pi}\right)^{m-n+1} n_{\sigma_1} \dots n_{\sigma_{m-n+1}}\right),$$

where the last equality holds because  $\frac{\gamma n_{\sigma_i}}{2\pi} - 1 \leq \left\lfloor \frac{\gamma n_{\sigma_i}}{2\pi} \right\rfloor \leq \frac{\gamma n_{\sigma_i}}{2\pi}$ , for every  $i \in \{1, \dots, m-n+1\}$ . Regarding part (iv), suppose that  $\Sigma = (\sigma_1, \dots, \sigma_{m-n+1})$  is the cycle basis obtained from modified Horton algorithm in [45]. Then the length of  $\Sigma$  is bounded above by  $3(n-1)(n-2)/2$  [27, Theorem 6]. Therefore, we have

$$n_{\sigma_1} \dots n_{\sigma_{m-n+1}} \leq \left(\frac{n_{\sigma_1} + \dots + n_{\sigma_{m-n+1}}}{m-n+1}\right)^{m-n+1} \leq \left(\frac{3(n-1)(n-2)}{2(m-n+1)}\right)^{m-n+1}.$$

As a result, by part (iii), the run time of the for-loop in steps 2-11: is  $\mathcal{O}\left(\log(\rho^{-1})n^3 \left(\frac{3(n-1)(n-2)}{m-n+1}\right)^{m-n+1}\right)$ . Moreover, the run time of the modified Horton algorithm in [45] is  $\mathcal{O}(m^2n/\log(n) + n^2m)$  (see Remark 3.2). Thus the result easily follows.  $\square$